Section A-Research Paper
ISSN 2063-5346

SYNTHESIS AND BIOLOGICAL EVALUATION OF NOVEL PEPTIDE ISOSTERES COMPOUNDS

[1]Pratibha Km (Research Scholar), [2]Yadav Preeti, [3]Bhardwaj Muskan
IIMT College of Medical Sciences, IIMT University Meerut
Email Id: Pratibhay803@gmail.com

Abstract
This study presents the synthesis and biological evaluation of novel peptide isosteres compounds aimed at developing effective antimicrobial agents. The compounds were designed, synthesized, and characterized using techniques such as nuclear magnetic resonance spectroscopy, mass spectrometry, and high-performance liquid chromatography to confirm their structural features and purity. Antimicrobial activity assays were conducted to evaluate their efficacy against a panel of pathogens, with minimum inhibitory concentration (MIC) and minimum bactericidal/fungicidal concentration (MBC/MFC) values determined. Cellular activity assays assessed cytotoxicity and selectivity towards mammalian cells. The results demonstrated varying levels of antimicrobial activity, with certain peptide isosteres exhibiting potent inhibitory effects against drug-resistant pathogens. The MIC values ranged from 6.25µg/mL to 50µg/mL, while the MBC/MFC values ranged from 12.5µg/mL to >50µg/mL. Importantly, the compounds displayed selectivity towards microbial cells, with low cytotoxicity towards mammalian cells. The findings provide insights into the structure-activity relationships of the peptide isosteres and their potential as therapeutic candidates. This study contributes to the field of peptide-based therapeutics by offering new avenues for combating antibiotic resistance and developing targeted antimicrobial therapies. The synthesized peptide isosteres hold implications for the development of alternative treatments for microbial infections, addressing the limitations of existing antimicrobial agents, and advancing the field of peptide-based research. These findings underscore the potential of peptide isosteres as promising candidates for the development of effective antimicrobial agents.

Keywords: Antimicrobial agents, Novel Peptide Isosteres Compounds, Minimum Inhibitory Concentration, Microbial Infections.

Introduction:

Peptides, composed of amino acids, are crucial players in a wide range of biological processes, including cellular signaling, enzyme regulation, and immune response modulation. Their unique properties make them attractive candidates for therapeutic interventions. However, the clinical utility of peptides is often hampered by challenges such as rapid degradation, limited stability, and poor bioavailability [1].

To address these limitations, the development of peptide isosteres has emerged as a promising strategy in the field of drug discovery.

Peptide isosteres are non-peptidic compounds that mimic the structural and functional properties of peptides while offering improved stability, enhanced pharmacokinetics, and increased oral bioavailability [2].

These isosteres are designed to replicate key features of peptides, such as specific backbone conformations, hydrogen bonding patterns, and critical amino acid side chains, allowing them to interact with biological targets in a similar manner to their peptide counterparts [3].

The rational design and synthesis of peptide isosteres involve modifying the peptide backbone or side chains to generate non-peptidic compounds that retain or even enhance the biological activity of the original peptide sequence [4].

Various chemical modifications can be applied, such as replacement of peptide bonds with amide isosteres, introduction of conformational constraints, incorporation of non-natural amino acids, or use of peptidomimetic scaffolds. These modifications aim to improve proteolytic stability, increase membrane permeability, and enhance target selectivity.

The field of peptide isosteres holds significant potential for the development of therapeutics targeting a wide range of diseases, including cancer, cardiovascular disorders, inflammatory diseases, and central nervous system disorders. By addressing the limitations of peptides, peptide isosteres offer opportunities to explore new avenues in drug design and delivery [5].

The synthesis and biological evaluation of novel peptide isosteres compounds present an exciting research endeavor, as it combines principles of organic chemistry, medicinal chemistry, and pharmacology. Through the design and synthesis of structurally diverse peptide isosteres, researchers can explore their physicochemical properties, assess their biological activities, and gain insights into their mechanism of action [6].

This research aims to contribute to the expanding knowledge base of peptide isosteres and pave the way for the development of novel therapeutic agents with improved pharmacological profiles and therapeutic efficacy [7].

Materials and Methods:

Synthesis Step	**Materials and Reagents**
For the synthesis of 2-(1-aminocyclohexyl) acetic acid, β3, 3-Ac6c:	
Starting Materials:	
- Cyclohexanone (7.70g, 50mmol)	- Malonic acid (5.20g, 50mmol)
- Ammonium acetate (11.55g, 150mmol)	- Ethanol (100mL)
Solvents and Reagents:	- Acetone (for extraction)
- Deuterated methanol (MeOD) (for NMR)	- Silica gel (60-120 mesh) for column chromatography
- 2N-HCl (hydrochloric acid) solution	- 2M-Na2CO3 (sodium carbonate) solution
- Saturated sodium chloride (brine) solution	- Anhydrous sodium sulfate
For the synthesis of Boc-Leu-β3, 3-Ac6c-OMe (P1):	
Starting Materials:	- Boc-Leu-OH (1.15g, 5.0mmol)
Solvents and Reagents:	- Dichloromethane (DCM)
- NMM (N-methyl morpholine) (1.5mL, 10.0mmol)	- EDC (0.95g, 5.0mmol)
- H2N-β3, 3Ac6c-OMe.HCl (1.03g, 5.0mmol)	- Ethyl acetate (for extraction)
- Silica gel (60-120 mesh) for column chromatography	- CDCl3 (for NMR)
- High-resolution mass spectrometry-electrospray ionization (HRMS-ESI)	

For the deprotection and coupling reactions:	
Reagents:	- Trifluoroacetic acid (TFA)
- Diethyl ether	Solvents:
Starting Materials:	- N,N-dimethylformamide (DMF)
- Boc-Leu-β3,3-Ac6c-OMe (0.768 g, 2.0mmol)	- Nitrogen atmosphere (for reactions under inert conditions)
- Boc-Leu-β3, 3-Ac6c-OH (0.74 g, 2.0mmol)	- Anhydrous sodium sulfate (for drying)
- Boc-(Leu-β3,3-Ac6c)2-OMe (P2)	- High-performance liquid chromatography (HPLC) equipment (for purification)
For the synthesis of Boc-(Leu-β3,3-Ac6c)2-OMe (P2):	
Solvents and Reagents:	- Ethyl acetate (for extraction)
- 2N hydrochloric acid (HCl) solution	- 2M sodium carbonate (Na2CO3) solution
- Saturated brine solution	- High-resolution mass spectrometry with electrospray ionization (HRMS-ESI)

Experimental Section:

All the chemicals required for the synthesis were purchased from Sigma Aldrich, Novabiochem, and Himedia. The solvents used in the reactions were purified by distillation and drying before use. Peptides P1-P4 was synthesized using conventional methods in a liquid solution. To protect the N-terminal, we used Boc group, while the C-terminal was protected as a methyl ester. The Boc group was removed using a solution of 30% tri-fluoroacetic acid (TFA) in dichloromethane (DCM). The coupling reactions were facilitated by using 1-ethyl-3(3, 3-dimethylaminopropyl carbodiimide hydrochloride (EDCI. HCl), 1-hydroxy-benzotriazole (HOBt), & N-methyl-morpholine (NMM) as a suitable base. Purification was carried out using column chromatography on silica gel (60-120mesh) and high-performance liquid chromatography (HPLC) on a reversed-phase semi-preparative C18 column (10×250mm, 10µ) with a gradient of methanol and water. The final peptides were characterized using high-resolution mass spectrometry (HRMS) on an Agilent Technologies 6540 instrument [8].

Synthesis of 2-(1-aminocyclohexyl) acetic acid ($C^{3,3}$-Ac_6c):

The compound β, β-disubstituted-β-amino acid, β3, 3-Ac6c, was synthesized following a procedure described in the literature (Wani et al., 2013).

In brief, a mixture of cyclohexanone (7.70 g, 50mmol), Malonic acid (5.20g, 50mmol), and ammonium acetate (11.55g, 150mmol) was added to 100ml of ethanol. The reaction mixture was refluxed for 24hours. After the reaction was complete, the mixture was allowed to cool to room temperature, and ethanol was removed under reduced pressure. The resulting residue was treated with acetone (3×50 ml) and dried, yielding a white solid of 2-(1-aminocyclohexyl) acetic acid, β3, 3-Ac6c, with a yield of 6.5 g (90%). The melting point of the compound was determined to be 265-267°C. The proton nuclear magnetic resonance (1H NMR) spectrum of the compound in deuterated methanol (MeOD) showed signals at δ 2.35 (singlet, 2H) and 1.75-2.1 (multiplet, 10H). High-resolution mass spectrometry-electrospray ionization (HRMS-ESI) analysis revealed calculated mass (MCal) of 157.14 & observed mass (MObs) of 158.16 [M+H]+.

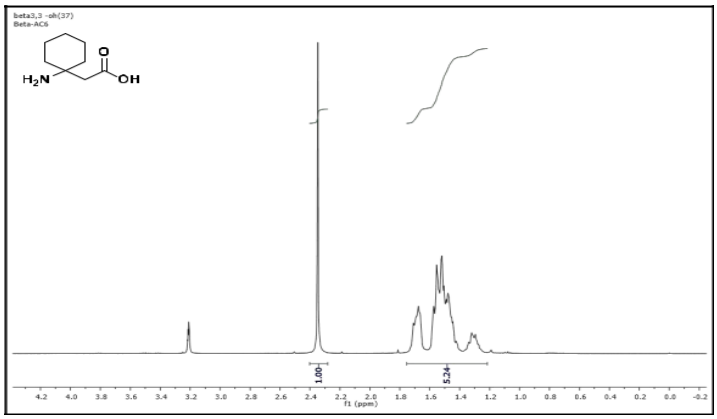

Fig.1: 400MHz ^{1}H NMR spectrum of $\beta^{3,3}$ Ac_6c, 2-(1-aminocyclohexyl)acetic acid ($C^{3,3}Ac_6c$) in CD_3OD

Synthesis of Boc-Leu-$\beta^{3,3}$-Ac_6c-OH, P1:

Scheme.1

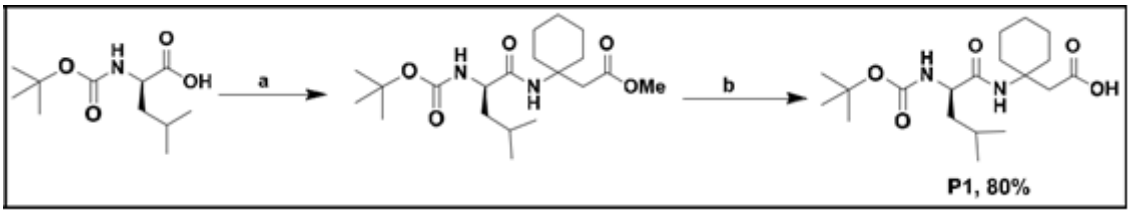

Boc-Leu-OH (1.15grams, 5.0millimoles) was dissolved in 3.0milliliters of dry DCM (dichloromethane) and cooled in an ice bath while stirring. NMM (N-methyl morpholine) (1.5 milliliters, 10.0millimoles) was added, followed by the addition of EDC (N-ethyl-N'-(3-dimethylaminopropyl) carbodiimide) (0.95grams, 5.0millimoles) and the amino acid ester hydrochloride H2N-β3, 3Ac6c-OMe.HCl (1.03grams, 5.0millimoles). The reaction mixture was allowed to reach room temperature and stirred for 16 hours. After the reaction was completed, which was monitored using TLC (thin-layer chromatography), the solvent was evaporated and the remaining substance was dissolved in ethyl acetate. The organic layer was washed with 2N-HCl (hydrochloric acid) solution (three times, 15milliliters each), 2M-Na2CO3 (sodium carbonate) solution (three times, 15milliliters each), and brine solution (saturated sodium chloride solution) (three times, 15milliliters each). The organic layer was dried with anhydrous sodium sulfate and evaporated under vacuum. The crude peptide acid was purified using column chromatography with silica gel (60-120mesh) to obtain Boc-Leu-β3, 3-Ac6c-OMe [9].

Boc-Leu-β3, 3-Ac6c-OMe (0.76grams, 2.0millimoles) was dissolved in 5.0milliliters of dry methanol and 2.0milliliters of 2N-NaOH (sodium hydroxide) was added. The reaction mixture was stirred for 3 hours. The reaction progress was monitored using TLC at regular intervals. The solvent was evaporated and the remaining substance was extracted with ethyl acetate. The aqueous layer was acidified using 2N-HCl and extracted with ethyl acetate (three times, 10milliliters each). The combined organic layer was evaporated under vacuum to obtain Boc-Leu-β3, 3-Ac6c-OH. It was further purified using column chromatography with silica gel (60-120 mesh) to yield Boc-Leu-β3, 3-Ac6c-OH, referred to as P1. The structure of P1 was confirmed using 1H NMR (proton nuclear magnetic resonance) spectroscopy (400 MHz, CDCl3), and its mass was determined using HRMS-ESI (high-resolution mass spectrometry-electrospray ionization). The results showed δ6.62 (singlet, 1H), 6.36 (singlet, 1H), 5.04 (singlet, 1H), 4.07 (multiplet, 1H), 2.83 (singlet, 2H), 2.19 (multiplet, 2H), 1.45 (singlet, 19H), 0.93 (doublet, J = 6.0 Hz, 6H). The calculated molecular weight (MCal) was 370.24, and the observed molecular weight (MObs) was 371.25 [M+H]+.

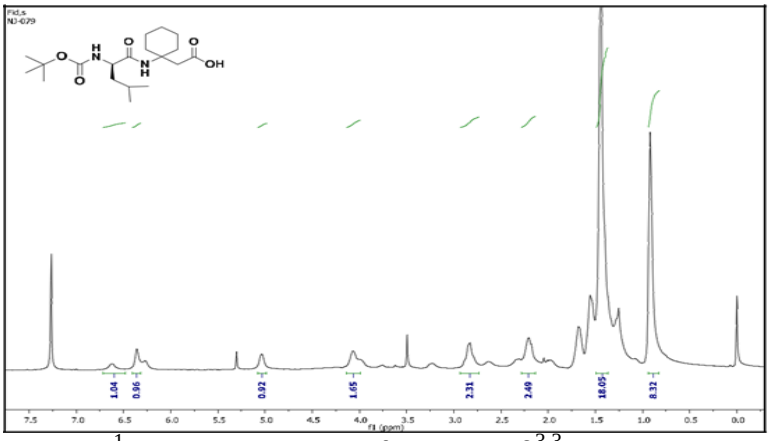

Fig.2: 400MHz ^{1}H NMR spectrum of Boc-Leu-$\beta^{3,3}$-Ac_6c-OH, **P1** in $CDCl_3$

Synthesis of Boc-(Leu-$\beta^{3,3}$-Ac_6c)$_2$-OMe, P2:
Scheme.2

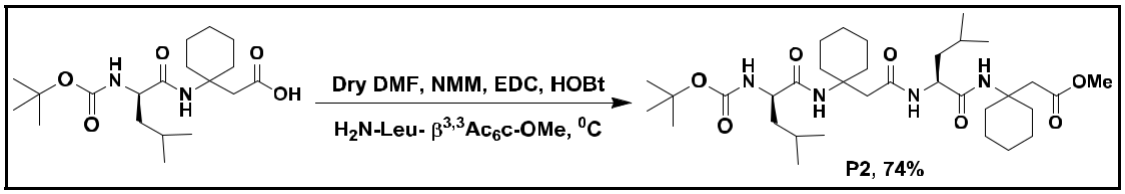

The compound Boc-Leu-β3,3-Ac6c-OMe (0.768 g, 2.0 mmol) was treated with 2.0 ml of a solution containing 30% trifluoroacetic acid (TFA) in dichloromethane (DCM) to remove the protecting group. The progress of the deprotection reaction was monitored using thin-layer chromatography (TLC). Once the deprotection was complete, the solvent was evaporated under reduced pressure and the resulting residue was mixed with diethyl ether. The free base form of the dipeptide was obtained.

Next, the dipeptide was added to a cooled solution of Boc-Leu-β3,3-Ac6c-OH (0.74 g, 2.0 mmol) in 2.0 ml of dry N,N-dimethylformamide (DMF). N-methylmorpholine (NMM) (0.5 ml, 5.0 mmol), 1-ethyl-3-(3-dimethylaminopropyl)carbodiimide (EDC) (0.38 g, 2.0 mmol), and 1-hydroxybenzotriazole (HOBt) (0.27 g, 2.0 mmol) were then added to the mixture. The reaction mixture was allowed to reach room temperature and stirred under a nitrogen atmosphere for 24 hours. The progress of the reaction was monitored using TLC. Once the reaction was complete, the solvent was evaporated under reduced pressure. The resulting residue was dissolved in ethyl acetate. The organic layer was washed sequentially with 2N hydrochloric acid (HCl) (3x10 ml), 2M sodium carbonate (Na2CO3) (3x10 ml), and saturated brine solution (1x10 ml). The organic layer was dried using anhydrous sodium sulfate and then evaporated under vacuum. This yielded the tetrapeptide, which was further purified using high-performance liquid chromatography (HPLC) to obtain Boc-(Leu-β3,3-Ac6c)2-OMe, referred to as P2.

The structure of P2 was confirmed using 1H nuclear magnetic resonance spectroscopy (NMR) (400 MHz, CDCl3). The NMR spectrum showed characteristic signals corresponding to different protons in the molecule. The compound's molecular weight was determined using high-resolution mass spectrometry with electrospray ionization (HRMS-ESI), confirming its identity as 636.44amu. The observed mass of 637.45 amu corresponded to the [M + H]+ ion in the mass spectrum [10-11].

Synthesis of Boc-(Leu-$\beta^{3,3}$-$Ac_6c)_2$-Leu-OMe, P3
Scheme.3

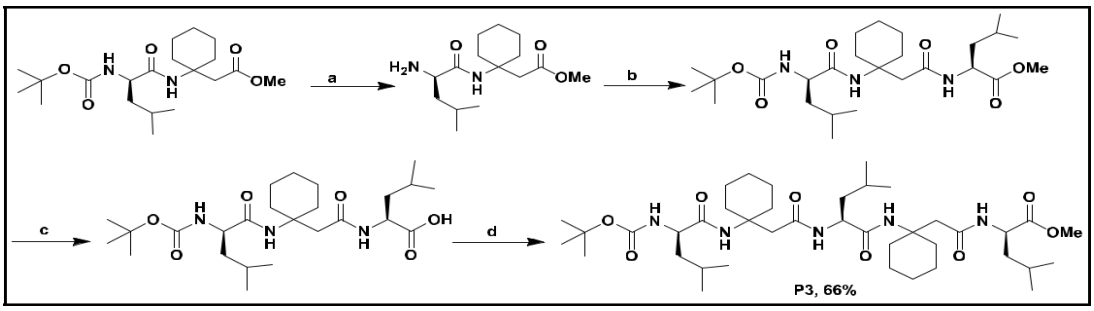

Reagents and conditions: (a) 30% TFA in DCM, 2 h; (b) Dry DCM, NMM, EDC, HOBt, Boc-Leu-OH, 0^0 C to rt, 16 h; (c) 2N-NaOH/MeOH, rt, 3 h; (d) Dry DMF, NMM, EDC, HOBt, H_2N-Leu-$c^{3,3}Ac_6c$-OMe, 0^0 C to rt, 24 h.

The compound Boc-Leu-β3, 3-Ac6c-OMe (0.768 g, 2.0mmol) was deprotected using 2.0 ml of a solution containing 30% trifluoroacetic acid (TFA) in dichloromethane (DCM). The progress of deprotection was monitored using thin-layer chromatography (TLC). Once the deprotection was complete, the solvent was evaporated under reduced pressure and the resulting residue was treated with diethyl ether. The resulting dipeptide free base was then added to a cooled solution of Boc-Leu-OH (0.462g, 2.0mmol) in 2.0ml of dry N, N-dimethylformamide (DMF). To this mixture, N-methylmorpholine (NMM) (0.5ml, 5.0mmol), 1-ethyl-3-(3-dimethylaminopropyl) carbodiimide (EDC) (0.38 g, 2.0 mmol), and 1-hydroxybenzotriazole (HOBt) (0.27 g, 2.0 mmol) were added. The reaction mixture was then stirred at room temperature for 24 hours under a nitrogen atmosphere. Once the reaction was complete, as monitored by TLC, the solvent was evaporated under reduced pressure. The resulting product, Boc-Leu-β3, 3-Ac6c-Leu-OMe, was obtained by following the described workup procedure (P2).

For the synthesis of Boc-(Leu-β3, 3-Ac6c) 2-Leu-OMe (P3), Boc-Leu-β3,3-Ac6c-Leu-OMe (0.497 g, 1.0 mmol) was deprotected using 1.0ml of a solution containing 30% TFA in DCM. The deprotection progress was monitored using TLC. Once de-protection was complete, the solvent was evaporated under reduced pressure and the resulting residue was treated with diethyl ether. The resulting dipeptide free base was then added to a precooled solution of Boc-Leu-β3,3-Ac6c-OH (0.37 g, 1.0mmol) in 1.0 ml of dry DMF. To this mixture, NMM (0.33 ml, 3.0 mmol), EDC (0.191 g, 1.0mmol), and HOBt (0.135 g, 1.0mmol) were added. The reaction mixture was allowed to reach room temperature and stirred for 48 hours under a nitrogen atmosphere. After the completion of the reaction, as monitored by TLC, the solvent was evaporated under reduced pressure. The resulting residue was dissolved in ethyl acetate. The organic layer was sequentially washed with 2N hydrochloric acid (3 × 10 ml), 2M sodium carbonate (3 × 10 ml), and saturated brine (1 × 10 ml). The organic layer was then dried using anhydrous sodium sulfate and evaporated under vacuum. The resulting pentapeptide was purified by high-performance liquid chromatography (HPLC) to yield Boc-(Leu-β3, 3-Ac6c) 2-Leu-OMe, designated as P3. The structure of P3 was confirmed using 1H nuclear magnetic resonance spectroscopy (NMR) (400 MHz, CDCl3) with the following peaks observed: δ 7.62 (d, J = 8.7 Hz, 1H), 6.56 (s, 1H), 6.50 (d, J = 5.5 Hz, 1H), 6.37 (s, 1H), 5.84 (d, J = 8.8 Hz, 1H), 4.63 (t, J = 8.5 Hz, 1H), 4.12 (td, J = 10.2, 4.1 Hz, 1H), 3.98 (d, J = 7.8 Hz, 1H), 3.65 (s, 3H), 2.95 (d, J = 12.5 Hz, 1H), 2.74 (d, J = 13.6 Hz, 2H), 2.39 (s, 1H), 2.08 (dd, J = 23.6, 12.5 Hz, 2H), 1.74 (s, 3H), 1.46 (m, 26H), 1.16 (m, 3H), 0.83 (m, 19H). The high-resolution mass spectrometry (HRMS-ESI) data showed the calculated mass (MCal) of 749.53 and the observed mass (MObs) of 750.53 [M + H]+ [12].

Synthesis of Boc-(Leu-$\beta^{3,3}$-$Ac_6c)_4$-OMe, P4:
Scheme.4

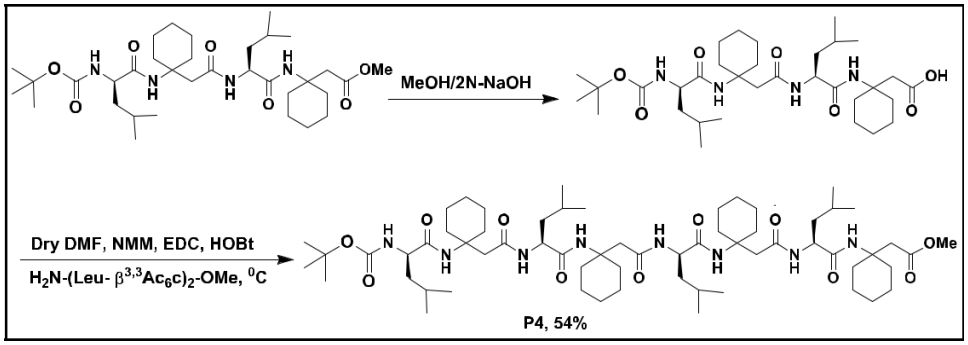

The peptide **P4** was synthesized by 4+4 coupling in solution phase. The free base H-(Leu-$\beta^{3,3}Ac_6c)_2$-OMe (0.321 g, 0.5 mmol) which was obtained by the deprotection of Boc-(Leu-$\beta^{3,3}$-$Ac_6c)_2$-OMe using 30% TFA in DCM was coupled with Boc-(Leu-$\beta^{3,3}$-$Ac_6c)_2$-OH (0.311 g, 0.5 mmol) according to procedure described for **P2** yielded **P4**, which was purified by HPLC as white solid.^{1}H NMR (400 MHz, $CDCl_3$): δ 8.25 (s, 1H), 7.33 (s, 1H), 7.24 (d, *J* = 8.7 Hz, 1H), 7.12 (s, 1H), 6.84 (s, 1H), 6.71 (s, 1H), 6.59 (s, 1H), 5.99 (d, *J* = 8.5 Hz, 1H), 4.58 (s, 1H), 4.32 (s, 1H), 4.23 (d, *J* = 8.4 Hz, 2H), 3.64 (s, 1H), 3.62 (s, 3H), 3.50 (d, *J* = 6.1 Hz, 1H), 3.34 (d, *J* = 16.4 Hz, 1H), 3.05 (dd, *J* = 20.3, 12.8 Hz, 3H), 2.84 (s, 1H), 2.77 (d, *J* = 11.8 Hz, 2H), 2.53 (d, *J* = 16.2 Hz, 2H), 2.38 (d, *J*=12.4,1H), 2.18–2.00 (m, 4H), 1.75 (s, 8H), 1.67–1.18 (m, 50H), 1.05–0.84 (m, 24H).HRMS−ESI: M_{Cal}=1140.81; M_{Obs}=1141.81[M + H]+.

Nuclear Magnetic Resonance:
All NMR experiments were carried out on a Bruker DRX-400, AV-500 and AV-400 spectrometer. Peptide concentrations of ~10mM in $CDCl_3$ were used for collecting NMR data for structure determination. Complete resonance assignment was achieved using a combination of Total correlation spectroscopy (TOCSY) (Braunschweiler *et al* 1983, Bax *et al* 1985) and Rotating-frame overhauser spectroscopy (ROESY) (Bothner-by *et al* 1984) experiments. 2D experiment was recorded in the phase-sensitive mode using TPPI method. 1024 data points were collected in the f2 dimension and 512 data points in the f1 dimension. NMR data were processed using the Bruker XWINNMR software. The data were zero-filled to 2K points in the f1 dimension and a shifted (π/2) sine-squared window function was applied to both the dimensions, prior to Fourier transformation. Hydrogen bonding information was obtained from $CDCl_3$-DMSO-d_6 titration experiments (Rai *et al* 2006, Sharma *et al* 2006).

Structure Calculations:
Structure calculation was done using a simulated annealing protocol in vacuum using DESMOND and OPLS 2005 force field with NOE constraints. A fully extended peptide molecule (all backbone dihedral angles were kept to be 180˚) was kept in orthorhombic simulation cell of dimensions 61.21*31.89*30.45 Å. In order to distinguish between theprochiral R and S alpha hydrogens, structure calculation was done by giving both the possible NOE restrains for any NOE assignment involving alpha hydrogens of beta residues. Upper limit for distance was kept at 2.5 Å, 3.5 Å and 5.0 Å for strong, medium and weak NOEs respectively except for OMe↔NH(6) (for which upper limit was kept 5 Å (between methyl carbon of OMe and NH(6). All the lower distance limits were taken to be 1.8 Å.

1Kcal/Mol force constant was used for all the constraints. The calculated 20 structures were superposed using MOLMOL (Koradi *et al* 1996).

X-ray diffraction:

The single crystals suitable for X-ray diffraction were obtained by slow evaporation of concentrated solutions in Methanol/water mixture (8:2 v/v). The intensity data was collected on a Bruker Kappa ApexII diffractometer (Mo Kα = 0.71073 Å) up to sin θ/λ = 0.654 by φ/ω scan. The initial unit cell was determined using a least squares analysis of a random set of reflections collected from three sets of 0.3º wide scans (12 frames per set) that were well distributed in reciprocal space. Data frames were collected with 0.3º wide scans, 30s per frame, in seven different sets with 3068 total fames by automated data collection strategy. The crystal-to-detector distance was kept at 6.0 cm. The final unit-cell parameters were obtained and refined using 4995 reflections. Bruker SMART (2008) software was used for data acquisition and Bruker SAINT+v7.34 software (2008) for data integration. Absorption corrections were applied using program SADABS (Sheldrick *et al* 1996). The experimental details of crystal data, data collection and structure solution are provided in Table.1.

The structure was solved by direct methods using SHELXT (Sheldrick *et al* 2015). All the non-hydrogen atoms of the peptide molecules could be located from the first E-map itself. They were refined first isotropically and then anisotropically. After this all the H atoms attached to carbon atoms of the molecules were fixed by geometric criteria. The rest of hydrogens of the molecule, which were involved in hydrogen bonding interactions, were located from successive difference Fourier maps and were refined isotropically. The refinements were carried out using SHELXL (Sheldrick *et al* 2008).The final refinement with all hydrogen atoms and the weighting scheme converged the R factor to 5.15 % (wR2 = 12.84%). Details of the refinement parameters are given in the Table.1 [13-14].

Table.1: Crystal and diffraction parameters for the peptides **P1**, **P2** and **P3**

S.No	**P1**	**P2**	**P3**
Empirical formula	C19H34N2O5	C34H60N4O7	C40H71N5O8.(C4H8O2)2
Formula weight	370.48	636.86	925.2
Crystal habit	Plates	Plates	Needles
Crystal size [mm]	0.3 × 0.17 × 0.09	1.01 × 0.195 × 0.04	0.7 × 0.25 × 0.16
Crystallizing solvent	methanol/water	ethyl acetate/hexane	dioxane/water
Temperature	293 K	130(2) K	100 K
Wavelength	0.71073 Å	0.71073 Å	0.71073 Å

Crystal system	Monoclinic	Orthorhombic	Orthorhombic
Space group	P21	P212121	P212121
Angles [α, β, γ]	α=90º, β=94.372(4)º, γ=90º	α=β=γ=90º	α=β=γ=90º
Volume [Å3]	2181.0 (3)	3766.4(12)	5332.6 (5)
Z	4	4	4
Density [g/cm3][calc.]	1.128	1.123	1.151
F(000)	808	1392	2016
Radiation	Mo Kα	Mo Kα	Mo Kα
θ Range [°]	1.454 to 27.526	2.162 to 27.717	1.734 to 27.464
Scan type	ω/φ	ω/φ	ω/φ
Independent reflections	9887	8693	12164
Measured reflections	33216	52745	72874
Observed reflections with I > 2σ (I)	4255	4272	9447
Rint	0.068	0.092	0.067
Δρmax / Δρmin [e Å-3]	0.13/-0.15	0.18/-0.18	0.42/−0.43

Goodness-of-fit on F2	0.938	0.951	1.023
Final R / wR2 [%]	0.052/1024	5.15/10.08	6.23/16.20
restraints / parameters	1/481	0/415	257/706
CCDC No.	1452938	1453070	1501355

Results and Discussion:

Conformational analysis by NMR:

Peptides **P2-P4** was readily soluble in non-polar organic solvent, $CDCl_3$. All the NMR experiments were carried out in $CDCl_3$. A combination of TOCSY and ROESY experiments were used for the complete assignment of all the resonances. Exposed and hydrogen bonded amide groups were identified by titrating the peptides in $CDCl_3$ against DMSO-d_6, maintaining constant peptide concentration. Secondary structure information was derived from the sequential d_{NN} and long range (*i*, *i*+2 and *i*, *i*+3) $d\alpha_N$ NOEs. The NMR parameters of peptides **P2-P4** are listed in Table.2.

Table.2: NMR parameters of peptides P2-P4

Residue	**δ (ppm)**	**3JNH-CαH (Hz)**	**Δδ (ppm)**
Peptide P2			
Leu (1)	5.26	7.83	1.32
β3,3Ac6c (2)	6.24	---	0.20
Leu (3)	6.62	4.18	0.76
β3,3Ac6c (4)	6.76	---	0.82
Peptide P3			
Leu (1)	5.89	8.85	0.40
β3,3Ac6c (2)	6.42	---	0.33
Leu (3)	6.55	5.80	0.74
β3,3Ac6c (4)	6.61	---	0.41
Leu (5)	7.66	8.75	0.18
Peptide P4			
Leu (1)	5.97	8.40	0.59
β3,3Ac6c (2)	6.68	---	0.35
Leu (3)	6.55	4.13	0.11
β3,3Ac6c (4)	7.30	---	0.31
Leu (5)	7.20	8.75	0.16
β3,3Ac6c (6)	6.82	---	0.30
Leu (7)	8.23	3.23	0.01
β3,3Ac6c (8)	7.10	---	-0.25

Backbone conformations of Boc-(Leu-$\beta^{3,3}$-Ac_6c)$_2$-OMe , P2:

^{1}H NMR spectrum obtained for peptide **P2** in $CDCl_3$ at 298K exhibits well-dispersed resonances, indicative of a folded structure. The ^{1}H NMR, TOCSY and ROESY spectra are shown in Figures.3-7.

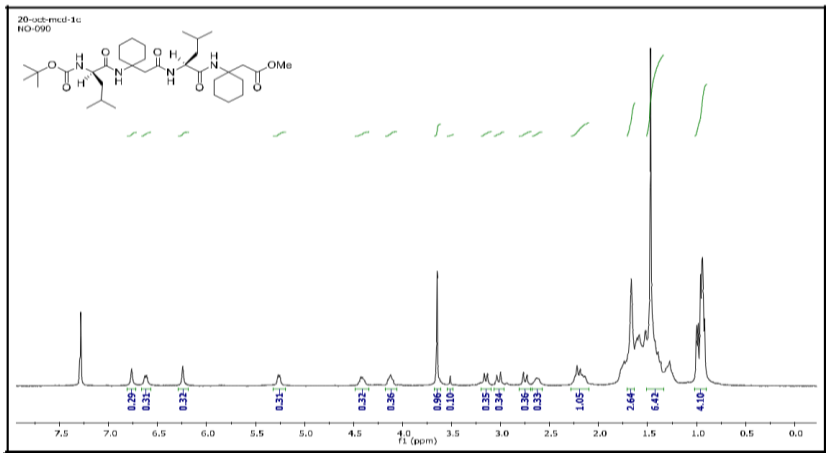

Fig.3: 400MHz ^{1}H NMR spectrum of Boc-(Leu-$\beta^{3,3}$-$Ac_6c)_2$-OMe, **P2** in $CDCl_3$ [15-17].

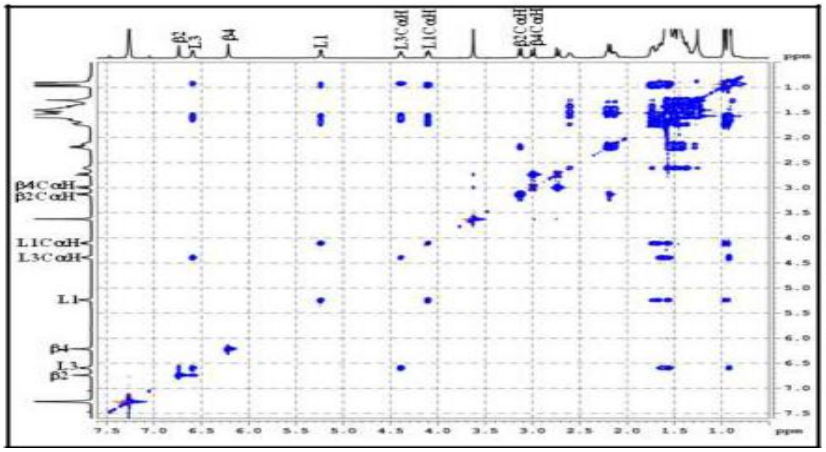

Fig.4: 500MHz TOCSY spectrum of Boc-(Leu-$\beta^{3,3}$-$Ac_6c)_2$-OMe, **P2** in $CDCl_3$

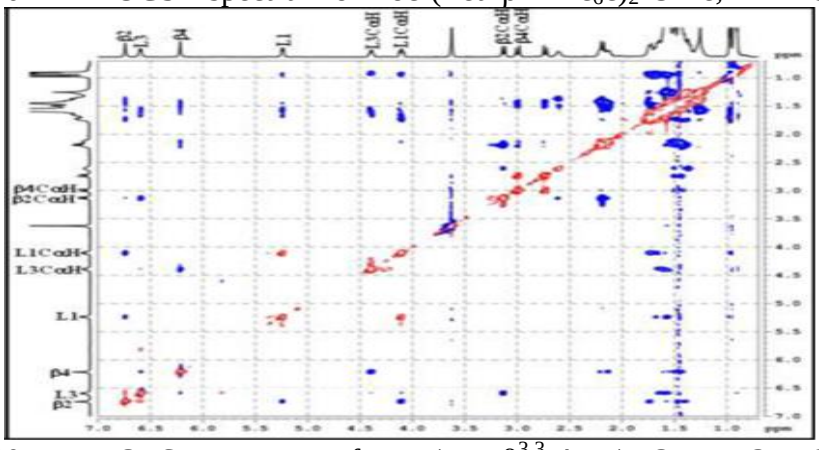

Fig.5: 500MHz ROESY spectrum of Boc-(Leu-$\beta^{3,3}$-$Ac_6c)_2$-OMe, **P2** in $CDCl_3$

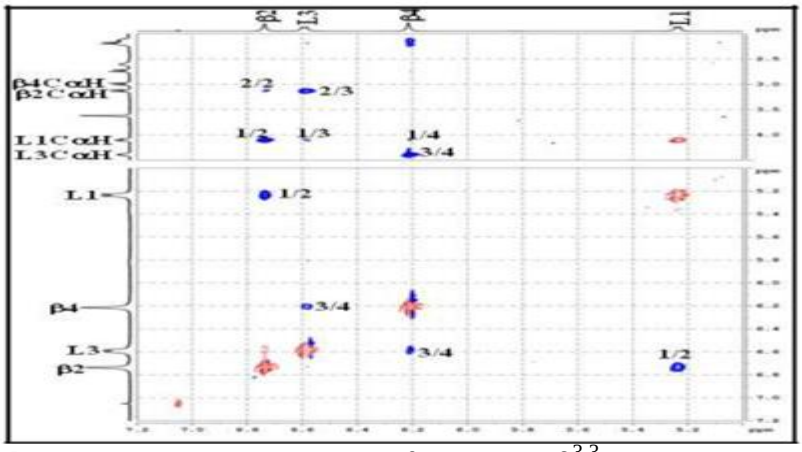

Fig.6: Partial 500MHz ROESY spectrum of Boc-(Leu-$\beta^{3,3}$-$Ac_6c)_2$-OMe, **P2** in $CDCl_3$ illustrating C$^{\alpha}$↔NH and NH↔NH NOEs.

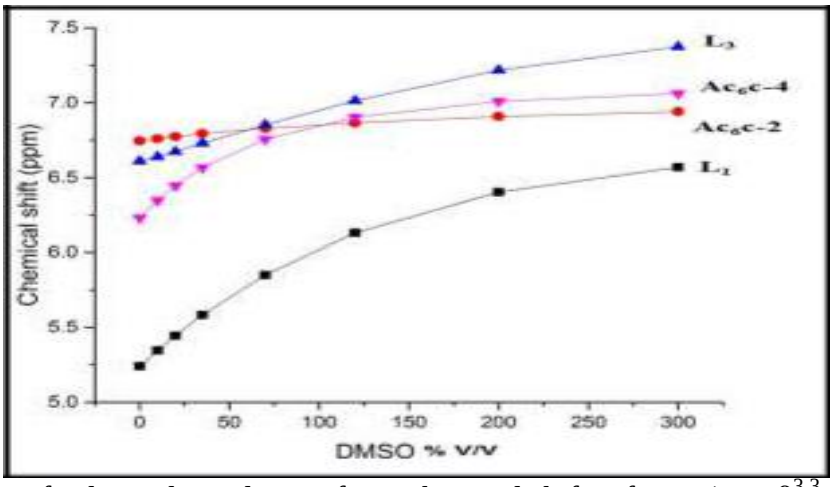

Fig.7: Plot of solvent dependence of NH chemical shifts of Boc-(Leu-$\beta^{3,3}$ $Ac_6c)_2$-OMe, **P2** at varying concentrations of DMSO-d_6 in $CDCl_3$.

Backbone conformations of Boc (Leu-$C^{3,3}$-$Ac_6c)_2$-Leu-OMe, P3:

Fig.3.4 shows the ^{1}H NMR spectrum obtained for peptide **P3** in $CDCl_3$ at 298K. The well-dispersed resonances indicate that peptide adopts folded structure. The TOCSY and ROESY spectra of peptide **P3** are shown in Fig.3.5 and 3.6. Fig.3.7 and 3.8 show partial C↔NH and N↔NH expansions of ROESY spectra. The backbone conformation of peptide **P3** was deduced from the observed NOEs between backbone NH and C^{α} H protons and the values of $^3J_{NH\text{-}C^{\alpha}H}$ coupling constants. The presence of strong intra-residue $d_{\alpha N}$ NOEs and weak inter-residue $d_{\alpha\ N}$ NOEs together with long range $d_{\alpha N}$ NOEs (*i*, *i*+2 and *i*, *i*+3) including Leu (3) CH↔Leu (5)NH, Leu (1) CH↔Leu (3)NH, Leu(1)C^2H↔$\beta^{3,3}$-Ac_6c(4)NH and $d_{N\alpha}$ $\beta^{3,3}$-Ac_6c(2)NH↔ $\beta^{3,3}$-Ac_6c(4)C^2H, Leu (1)NH↔ $\beta^{3,3}$-Ac_6c(4)CH and strong d_{NN} NOEs $\beta^{3,3}$-Ac_6c(4)↔Leu (5), Leu (1)↔$\beta^{3,3}$-Ac_6c(2), Leu(1)↔$\beta^{3,3}$-Ac_6c(4) suggests that the peptide **P3** adopts a helical conformation (Figures .8 & 9) [18-20].

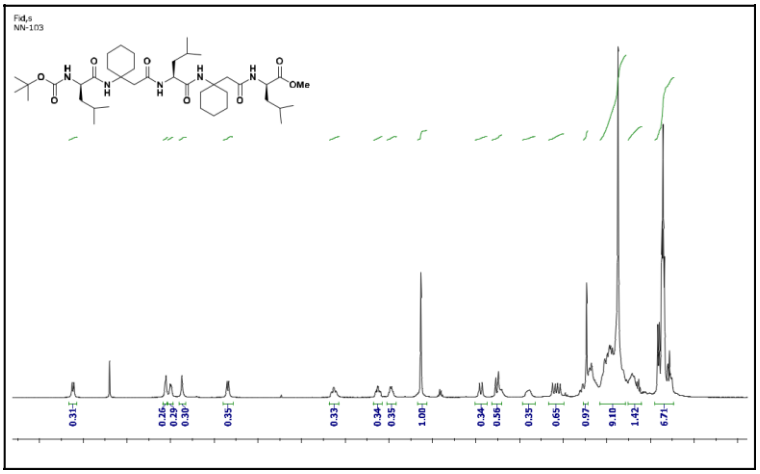

Fig.8: 400MHz ^{1}H NMR spectrum of Boc-(Leu-$\beta^{3,3}$-$Ac_6c)_2$-Leu-OMe, **P3** in $CDCl_3$

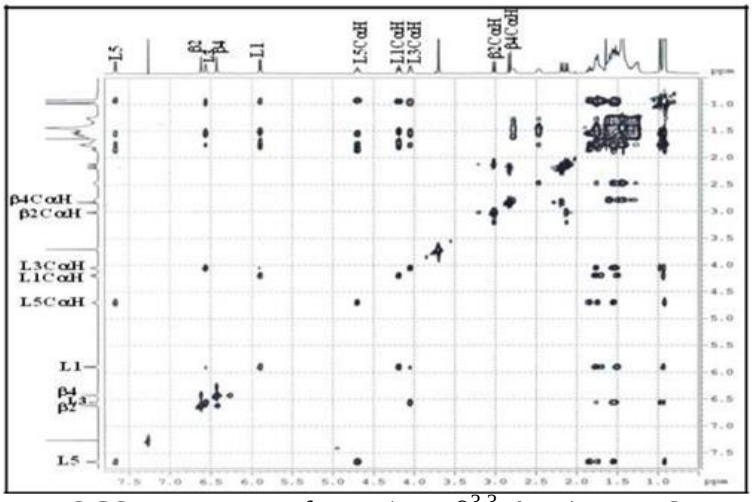

Fig.9: 500MHz TOCSY spectrum of Boc-(Leu-$\beta^{3,3}$-$Ac_6c)_2$-Leu-OMe, **P3** in $CDCl_3$

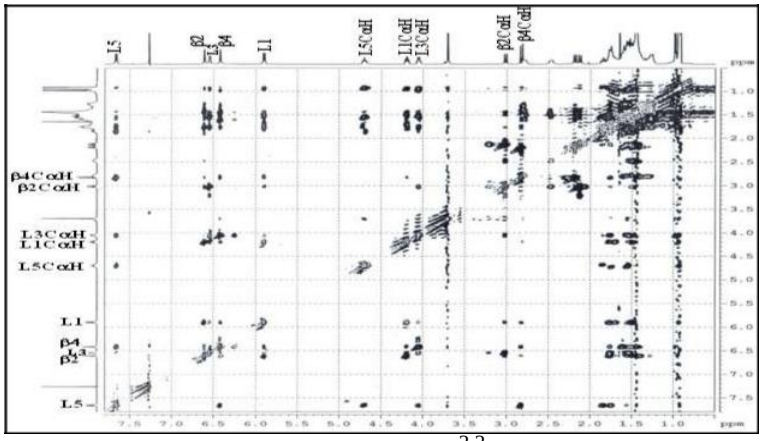

Fig.10: 500MHz ROESY spectrum of Boc-(Leu-$\beta^{3,3}$-$Ac_6c)_2$-Leu-OMe, **P3** in $CDCl_3$

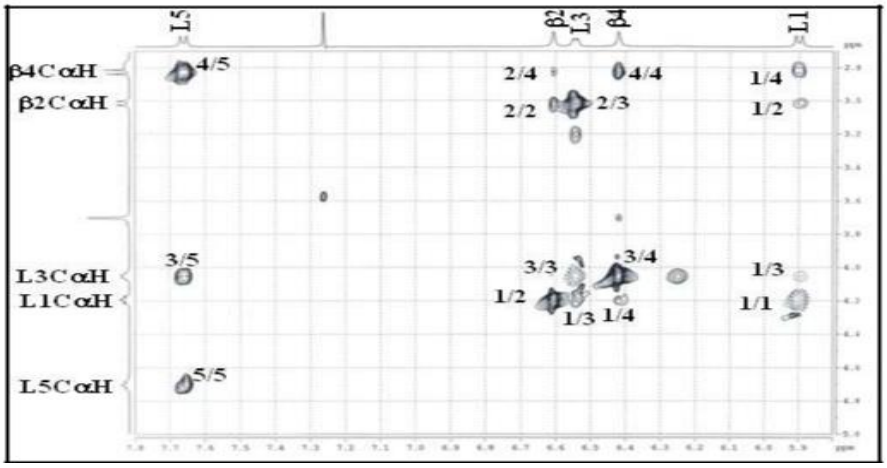

Fig.11: Partial 500MHz ROESY spectrum of Boc-(Leu-$\beta^{3,3}$-$Ac_6c)_2$-Leu-OMe, **P3** in $CDCl_3$ illustrating C↔NH NOEs

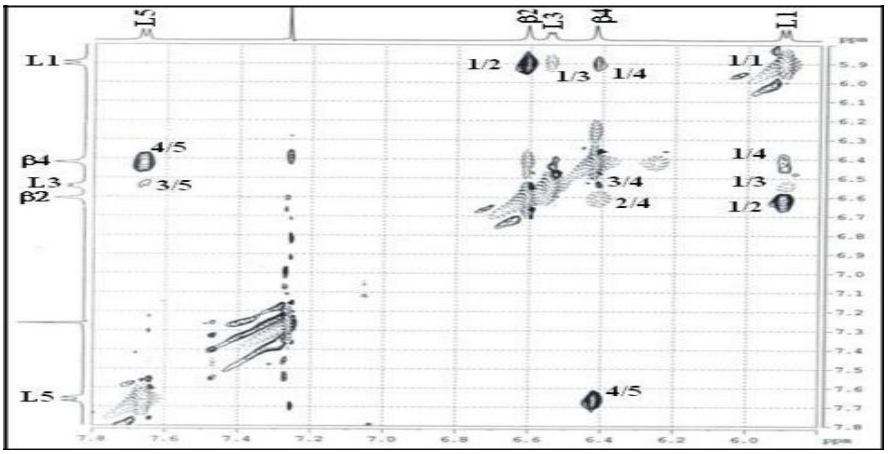

Fig.12: Partial 500MHz ROESY spectrum of Boc-(Leu-$\beta^{3,3}$-$Ac_6c)_2$-Leu-OMe **P3** in $CDCl_3$ illustrating NH↔NH NOEs.

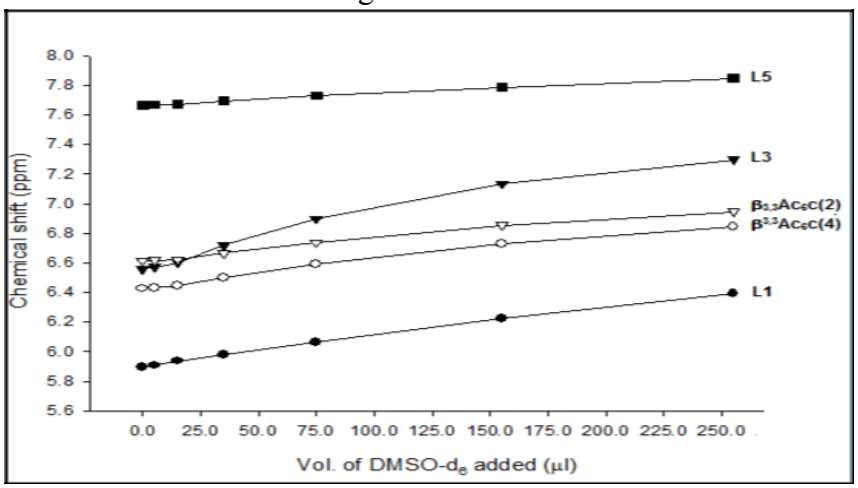

Fig.13: Plot of solvent dependence of NH chemical shifts of Boc-(Leu-$\beta^{3,3}$-$Ac_6c)_2$-Leu-OMe, **P3** at varying concentrations of DMSO-d_6 in $CDCl_3$.

Backbone conformations of Boc-(Leu-$\beta^{3,3}$-$Ac_6c)_4$-OMe, P4:

Fig.14 shows the ^{1}H NMR spectrum of peptide **P4** in $CDCl_3$ at 298K. The observation of well-dispersed resonances is indicative of a well-folded structure. The large values of $^3J_{HN\text{-}C^{\alpha}H}$ corresponding to Leu (1) and Leu (5) residues indicate the semi-extended conformation. The 700MHz TOCSY and ROESY spectra are shown in Fig.15, 16, 17 and 18 show partial C↔NH and N↔NH expansions of ROESY spectrum of the peptide **P4**. Examination of the ROESY spectrum (Fig.19) reveals the presence of several sequential d_{NN} NOEs, strong intra-residue self (*i-1*) d_N (N*i*H↔C*i*H) NOEs and weak sequential (*i, i+1*) d_N (C*i*H↔N*i+1*H) NOEs suggestive of helical conformation. In addition, long range $d_{\alpha N}$ and $d_{N\alpha}$ NOEs (*i, i+1*, *i, i*+2 and *i, i*+3) are observed which includes $\beta^{3,3}$ -Ac_6c (2) CH↔Leu (3)NH, Leu (3) CH↔$\beta^{3,3}$-Ac_6c (4) NH, Leu (5)CH↔$\beta^{3,3}$-Ac_6c (6) NH and $\beta^{3,3}$-Ac_6c(4) NH↔$\beta^{3,3}$-Ac_6c (8) CH and Leu (5) NH↔$\beta^{3,3}$-Ac_6c (8)C^2H are also observed (Fig.3.16). Strong d_{NN} NOEs are observed between Leu (1)↔$\beta^{3,3}$-Ac_6c (2), Leu (5)↔$\beta^{3,3}$-Ac_6c (6), $\beta^{3,3}$-Ac_6c (4)↔Leu (7), Leu (3)↔$\beta^{3,3}$-Ac_6c (8), Leu (5)↔$\beta^{3,3}$-Ac_6c (8). The presence of diagnostic NOEs like *i, i+2* and *i, i+3* is indicative of C_{11} helical conformation of the peptide (Hayen *et al* 2004). The solvent titration experiment of peptide **P4** shows that most of the amide resonances are largely invariant upon addition of DMSO-d_6 to a $CDCl_3$ solution, suggesting that they are involved in strong internal hydrogen bonds and favour helical conformation [21-23].

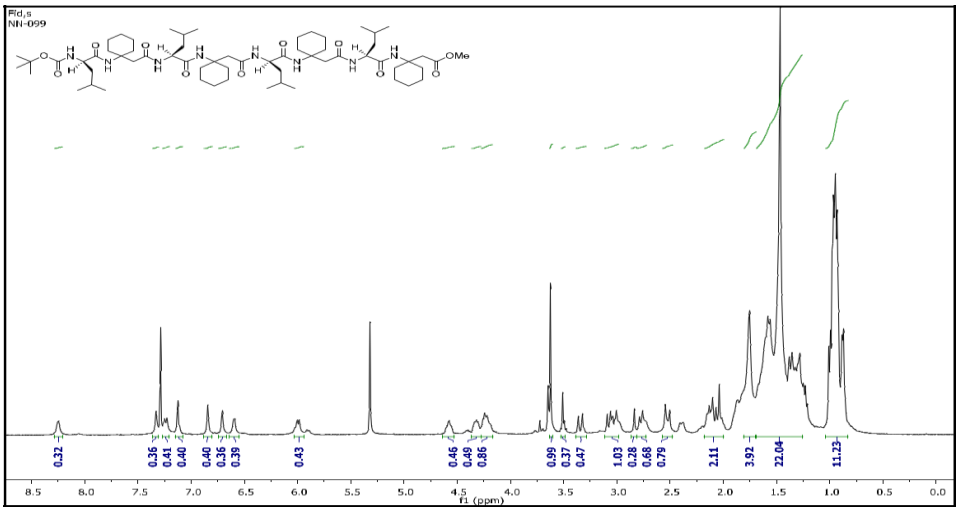

Fig.14: 400MHz^{1}HNMR spectrum of Boc-(Leu-$\beta^{3,3}$-$Ac_6c)_4$-OMe, **P4** in $CDCl_3$

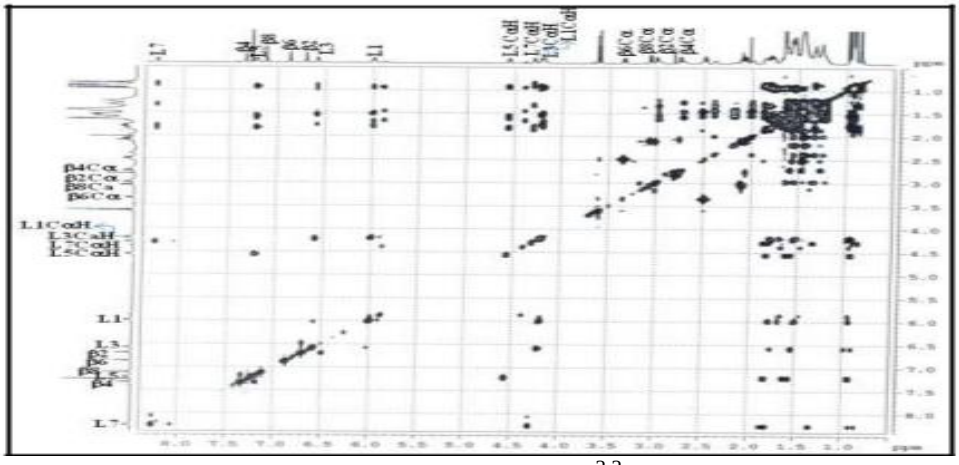

Fig.15: 700MHz TOCSY spectrum of Boc-(Leu-$\beta^{3,3}$-$Ac_6c)_4$-OMe, **P4** in $CDCl_3$

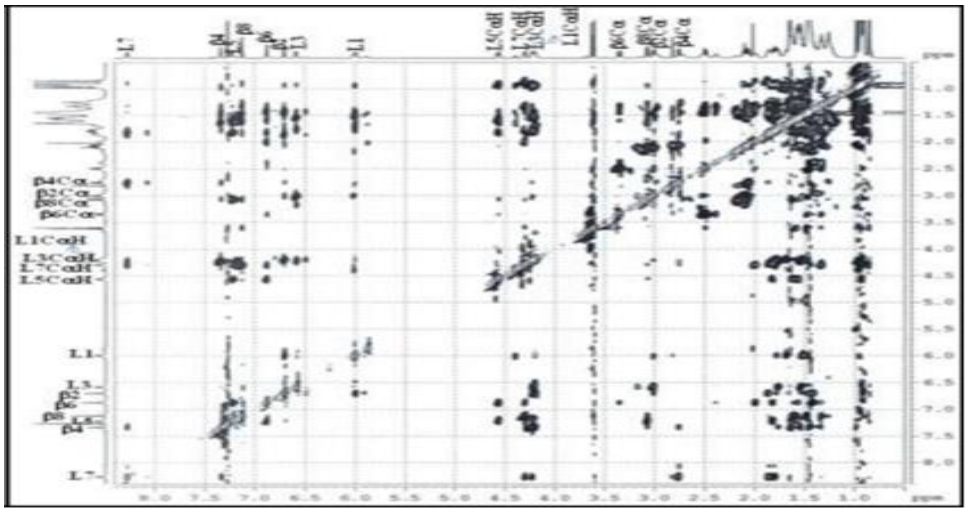

Fig.16: 700MHz ROESY spectrum of Boc-(Leu-$\beta^{3,3}$-$Ac_6c)_4$-OMe, **P4** in $CDCl_3$

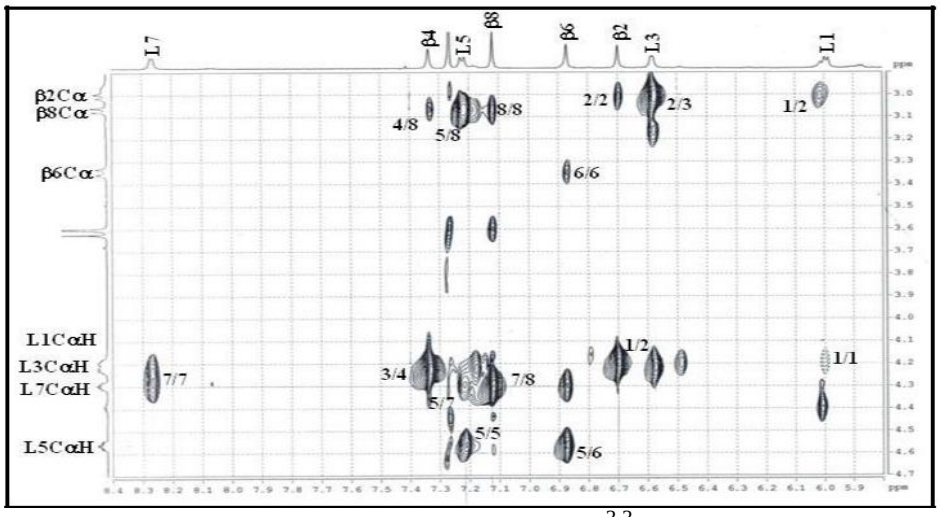

Fig.17: Partial 700MHz ROESY spectrum of Boc-(Leu-$\beta^{3,3}$-$Ac_6c)_4$-OMe**, P4** in $CDCl_3$ illustrating C↔NH NOEs

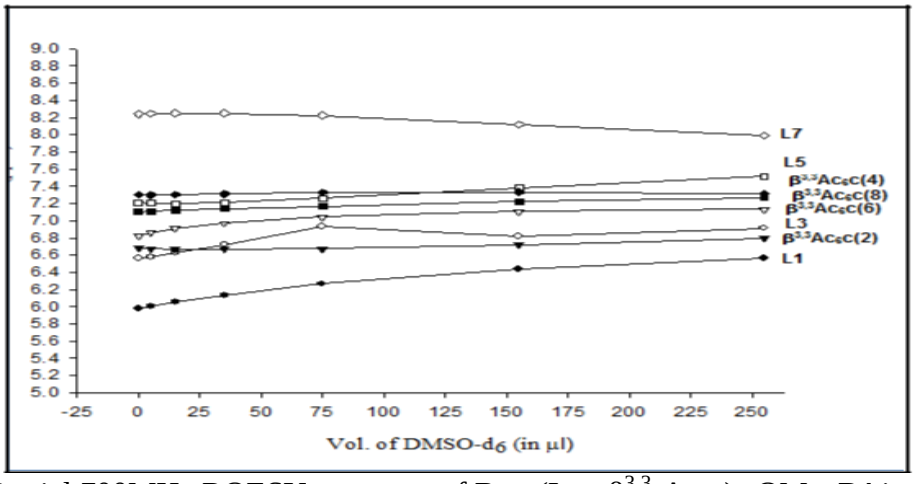

Fig.18: Partial 700MHz ROESY spectrum of Boc-(Leu-$\beta^{3,3}$-$Ac_6c)_4$-OMe, **P4** in $CDCl_3$ illustrating NH↔NH NOEs

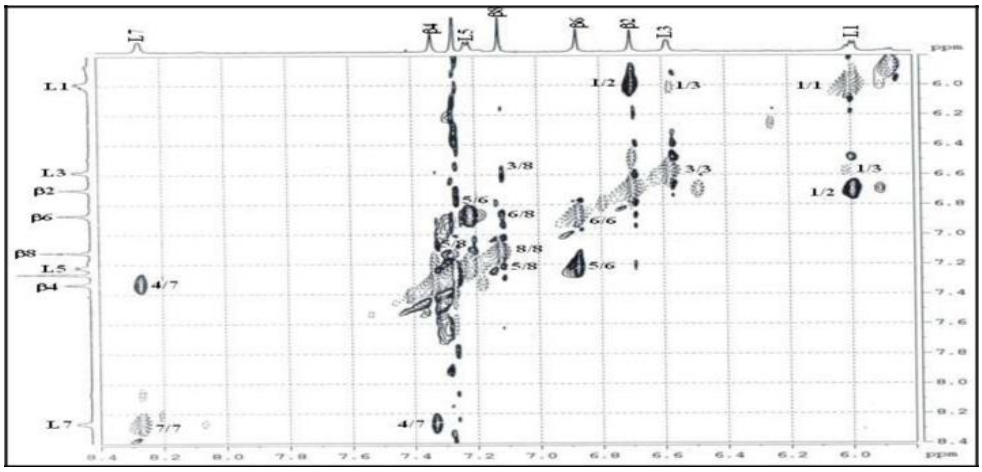

Fig.19: Plot of solvent dependence of NH chemical shifts of Boc-(Leu-$\beta^{3,3}$-$Ac_6c)_4$-OMe, **P4** at varying concentrations of DMSO-d_6 in $CDCl_3$.

NMR structure of Boc-(Leu-$\beta^{3,3}$-$Ac_6c)_4$-OMe, P4:

Structure calculation was done using a simulated annealing protocol in vacuum using DESMOND and OPLS 2005 force field with NOE constraints, which are listed in Table.3. A fully extended peptide molecule (all backbone dihedral angles were kept to be 180˚) was kept in orthorhombic simulation cell of dimensions 61.21*31.89*30.45 Å. In order to distinguish between the prochiral R and S alpha hydrogens, structure calculation was done by giving both the possible NOE restrains for any NOE assignment involving alpha hydrogens of beta residues. Upper limit for distance was kept at 2.5 Å, 3.5 Å and 5.0 Å for strong, medium and weak NOEs respectively except for OMe↔NH (6) (for which upper limit was kept 5 Å (between methyl carbon of OMe and NH(6). All the lower distance limits were taken to be 1.8 Å. 1 Kcal/Mol force constant was used for all the constraints. 20 minimum energy structures were taken from the trajectory between 1000 ps and 1200ps and minimized using a steepest descent method using a convergence gradient threshold of 0.5kcal/mol/Å. Analysis of the minimized structure didn't show any significant NOE restrain violations. The calculated 20 structures were superposed using MOLMOL (Koradi *et al* 1996) shown in Fig.20 [24].

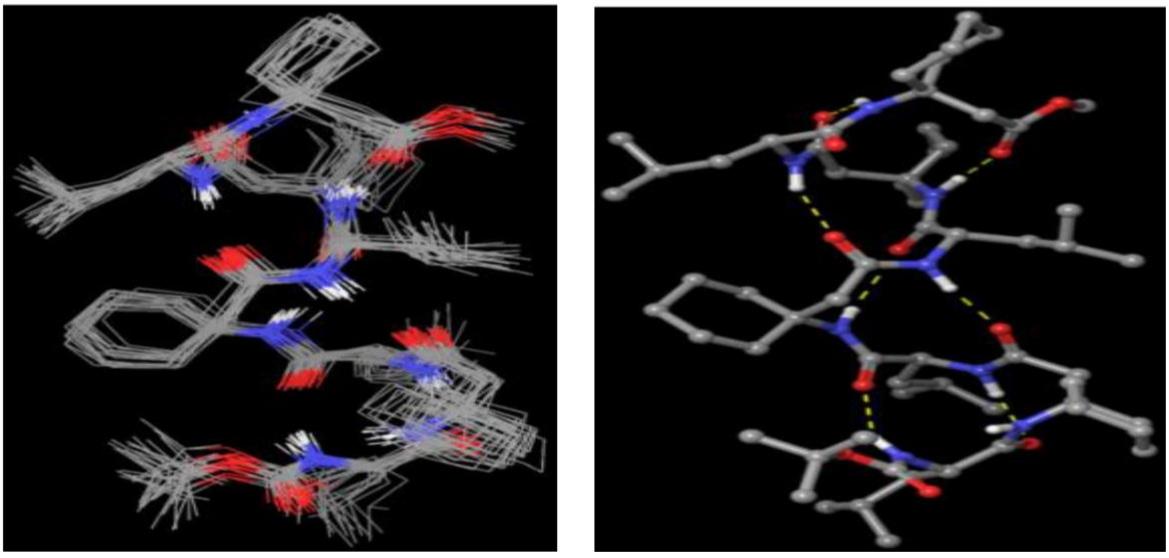

Fig.20: Superposition of 20 minimum energy structures taken from the trajectory between 1000 ps and 1200 ps of simulated annealing (left) and minimized lowest energy structure

(right). (Structures are taken from the second simulated annealing in which only correct NOE restrains are used) [25].

X-ray studies of peptides P1-P3:

Single crystals of **P1, P2** and **P3** were obtained by slow evaporation of methanol/water (9:1), ethyl acetate/hexane (8:2) and dioxane/water (8:2), respectively. **P1** was crystallized in monoclinic space group $P2_1$ with two molecules in the asymmetric unit. Peptides **P2** and **P3** were crystallized in orthorhombic space group $P2_12_12_1$. The molecular conformation of **P1**-**P3** as determined in the crystals are shown in Fig.21.

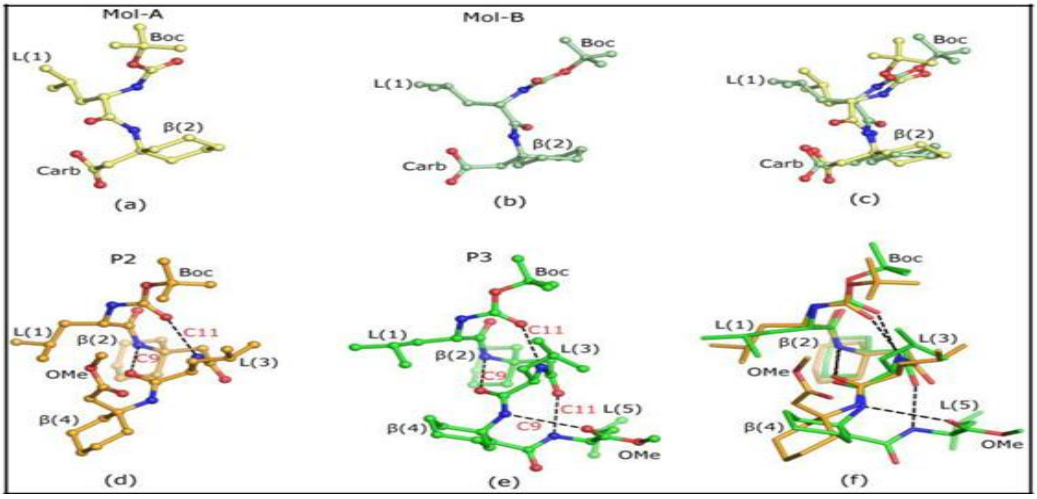

Fig.21: The solid state molecular conformations of (**a-b**) Boc-Leu-$\beta^{3,3}$-Ac_6c-OH, **P1** showing two independent molecules A and B respectively; (**c**) superposition of the two molecules of **P1** (**d**) Boc-Leu- $\beta^{3,3}$-Ac_6c-Leu-$\beta^{3,3}$-Ac_6c-OMe, **P2** (golden colour) showing C_{11}/C_9 intramolecular hydrogen bonds and (**e**) Boc-Leu-$\beta^{3,3}$-Ac_6c-Leu-$\beta^{3,3}$-Ac_6c-Leu-OMe, **P3** (green colour) showing C_{11}/C_9 intramolecular hydrogen bonds. (**f**) The super position of **P2** and **P3**. Hydrogen bonds are shown by dashed lines. All the H atoms are removed for sake of clarity.

The observed backbone torsion angles and hydrogen bond parameters are listed in Tables.3 and 6, respectively. Peptide **P1** exhibits the extended conformation for both the molecules A and B. The intra molecular hydrogen bond is not observed in either molecules of **P1**-Ac_6c residue in **P1** adopts *gauche* conformation with positive (+) and negative (-) signs about C-C bond. The superposition of two independent molecules A and B (Fig.22c) shows that the structure of **P1** is quite flexible. Leu (1) in both the molecules adopts helical conformations [Mol. A=-105.1(5)º; ψ=-44.7(5)º, Mol. B:=-102.1(5)º, ψ=129.5(4)º].

Table.3: Torsional angles (deg) for peptides **P1**-**P3**

Residue	φ	θ	Ψ	ω
P1				
Molecule A				
Leu (1)	-105.1(5)	---	-44.7(5)	-175.5(4)
$\beta^{3,3}Ac_6c(2)$	59.4(5)	64.4(5)	---	---
Molecule B				
Leu (1)	-102.1(5)	---	129.5(4)	171.6(4)
$\beta^{3,3}Ac_6c(2)$	-61.2(5)	-65.8(5)	---	---

P2				
Leu (1)	-66.9(4)	---	143.2(3)	-173.7(3)
$\beta^{3,3}Ac_6c$(2)	79.0(4)	67.5(4)	-82.2(4)	159.0(3)
Leu (3)	-82.6(4)	--	156.9(3)	170.3(3)
$\beta^{3,3}Ac_6c$(4)	-56.9(4)	-44.6(4)	137.8(3)	---
P3				
Leu (1)	-52.9(4)	---	161.5(3)	-158.6(3)
$\beta^{3,3}Ac_6c$(2)	68.7(4)	58.8(4)	-95.0(4)	167.1(3)
Leu (3)	-58.5(4)	---	152.9(3)	-174.8(3)
$\beta^{3,3}Ac_6c$(4)	69.2(4)	64.0(4)	-87.6(4)	170.9(3)
Leu (5)	-86.5(4)	---	177.5(3)	---

Peptide **P2** folds into helical conformation stabilized by intra molecular C_{11} and C_9 hydrogen bonds (Fig.22d). C_{11} hydrogen bond forms between CO moiety of Boc group and NH of Leu (3) residue. The formation of C_9 hydrogen bond is observed between NH of $C^{3,3}$-Ac_6c (2) and CO of Leu (3). Leu (1) and Leu (3) residues adopt polyproline like conformation: Leu (1): C=-66.9^0,=143.2^0; Leu (3):-82.6^0 C=156.9^0. C_{11} and C_9 hydrogen bonds can be described as non helical turn due to polyproline conformation of Leu residues. The polyproline conformation for C-amino acid has already been characterized in CH hybrid peptides sequences (Basuroy *et al* 2012, Basuroy *et al* 2014).

Table.4: Hydrogen bond parameters for peptide P1-P3

Type	**Donor**	**Acceptor**	**D⋯A**	**H⋯A**	**D-H⋯A**
P1					
Intermolecular	N6A	O5B	2.983(5)	2.14	165
	N13A	O5B	3.304(6)	2.46	168
	O23A	O12Aa	2.717(6)	1.95	156
	N6B	O22Bb	2.996(6)	2.15	169
	N13B	O5A	2.945(6)	2.11	163
	O23B	O12Bc	2.591(5)	1.80	160
P2					
Intramolecular	N3	O2	2.991(3)	2.15	159
(C11, 4→1)					
Intramolecular	N2	O5	2.915(3)	2.14	147
(C9, 1→2)					
Intermolecular	N1	O4d	2.966(3)	2.09	176
Intermolecular	N4	O3e	2.901(4)	2.02	176
P3					
Intramolecular	N23	O6	2.966(4)	2.11	164
(C11, 4→1)					
Intramolecular	N14	O29	3.073(4)	2.48	125
(C9, 1→2)					
Intramolecular	N39	O22	2.854(4)	2.05	151
(C11, 4→1)					
Intramolecular	N30	O46	3.257(4)	2.65	127

(C9, 1→2)					
Intermolecular	N7	O38f	2.871(4)	2.06	153

The table provides a summary of various intermolecular and intra molecular interactions observed in the given data. The interactions are categorized into three groups: P1, P2, and P3. In P1, which represents intermolecular interactions, several donor-acceptor pairs are identified. For example, N6A acts as a donor to O5B, with a distance of 2.983 Å between them. Similarly, other donor-acceptor pairs such as N13A-O5B, O23A-O12Aa, N6B-O22Bb, N13B-O5A, and O23B-O12Bc are listed along with their respective distances and angles.

P2 focuses on intra molecular interactions. Specifically, the interactions involving N3-O2 (C11, 4→1) and N2-O5 (C9, 1→2) are mentioned. The distances between the donor and acceptor atoms, denoted as D···A, as well as the H···A distances and D-H. A angles are provided.

P3 continues with intra molecular interactions, featuring additional cases such as N23-O6 (C11, 4→1), N14-O29 (C9, 1→2), N39-O22 (C11, 4→1), N30-O46 (C9, 1→2), and N7-O38f. Similar to the previous sections, the distances, H···A distances, and D-H···A angles are specified.

Overall, the table offers a concise overview of the types of interactions, the participating donor and acceptor atoms, their distances, H···A distances, and D-H···A angles observed in the given data.

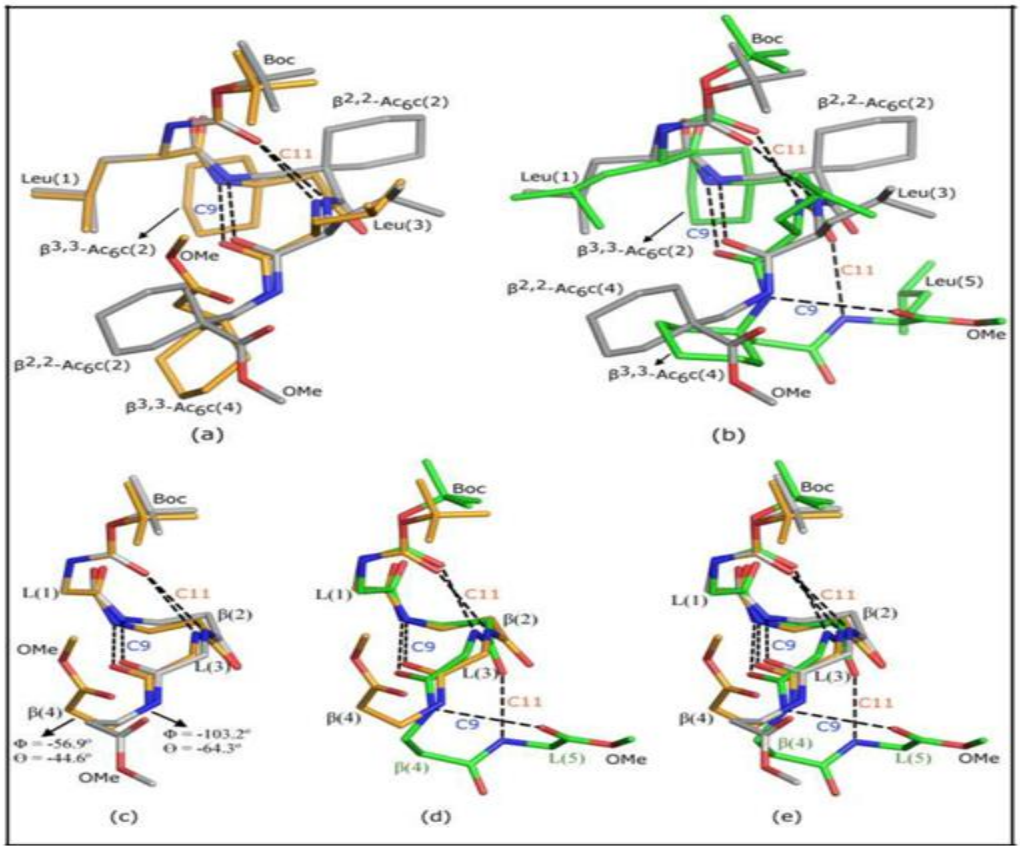

Fig.22: Comparison of molecular conformations (**a**) Tetrapeptide **P2** (golden color) with a related tetra peptide Boc-Leu-$\beta^{2,2}$-Ac_6c-Leu-$\beta^{2,2}$-Ac_6c-OMe (Basuroy *et al* 2014) shown in grey color (**b**) Penta peptide **P3** (green color) with the same related peptide.The relative backbone conformations of (c) tetra peptide **P2** with CCDC-988393, (**d**) tetra petide **P2** with pentapeptide **P3** and (**e**) all above three peptide together. The H atoms in all figures and side chain atoms in fig(**c-e**) are removed for the sake of clarity.

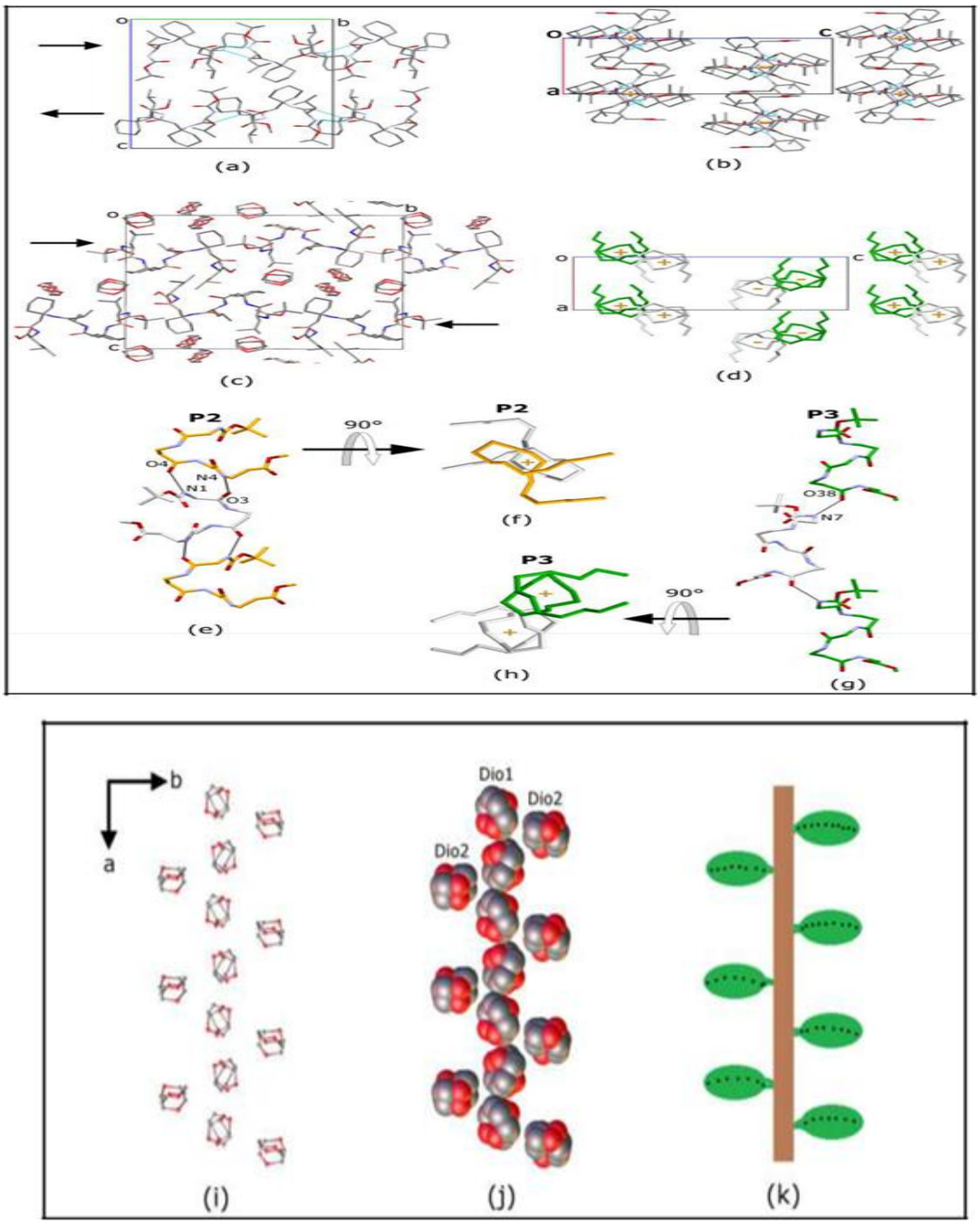

Fig.23: a, b, c, d, e, f, g, h, I, j, k provides a visual representation of the packing of molecules in crystals for P2 and P3, as well as the arrangement of helices and solvent molecules. The figure includes different views and annotations to enhance clarity.(a) and (b) depict the packing of P2 molecules in crystals, viewed along the a-axis and b-axis, respectively.(c) shows the packing of P3 molecules viewed along the a-axis, while (d) displays the packing of the helices of P3 viewed along the b-axis. In (d), the stick model is represented in green and grey colors, with side chains, carbonyls, and solvent molecules removed for better visibility. The (+) and (-) signs indicate the direction of the helix-axis, either pointing inwards into the plane of the paper or outwards towards the viewer. (e) and (f) present a side view and a top view, respectively, of the symmetry-related interconnected helices of P2. The helices are depicted in orange and grey (g) and (h) show a side view and a top view, respectively, of the symmetry-related interconnected helices of P3. The helices are

depicted in green and grey. Dotted lines in the figures indicate putative hydrogen bonds.(i) illustrates the stick model of the arrangement of disordered solvent molecules (Dioxane) within the crystals of P3.(j) presents a space-filling model of the same arrangement, where the solvent molecules are labeled as Dio1 and Dio2.(k) provides a cartoon diagram, resembling leaves arranged around a twig, to explain the arrangement of solvents in the crystals of P3 [26].

Short Hybrid Peptides Incorporating and Amino Acids as Antimicrobial Agents:

All the reagents for chemical synthesis were obtained from Sigma Aldrich, Novabiochem and Alfa aesar. The anhydrous solvents were purchased from Sigma Aldrich and Fisher Scientific. The reactions were monitored using thin-layer chromatography (TLC) on 0.25mm silica gel 60 F_{254} plates coated on aluminium sheet (E. Merck) and visualized using UV light (254nm) and ninhydrin as developing agent. The coupling reactions were mediated by 1-ethyl-3-(3-dimethylaminopropyl) carbodiimide hydrochloride (EDCI. HCl) /1-hydroxybenzotriazole (HOBt) in dry di-methylformamide (DMF)/or dry di-chloro methane (DCM) in presence of N-methylmorpholine (NMM). Purification of compounds was carried out by column chromatography using silica gel 60-120 mesh stationary phase.^{1}H NMR and^{13}C NMR spectra (with chemical shifts expressed in δ and coupling constants in Hertz) were recorded on Bruker DPX, 400 instruments using $CDCl_3$ as the solvents with TMS as internal standard. High resolution mass spectra (HRMS) were recorded on Agilent Technologies 6540 instrument [27-28].

Synthesis of Disubstituted amino acid:

The Disubstituted amino acids, c_6c and Pip (Ac) were synthesised according to the procedure reported in literature (Wani *et al* 2013).

Synthesis of Mono-substituted Amino acids, Boc-C^{4}-L-Phe-OH/ Boc-C^{4}-L-Leu-OH:

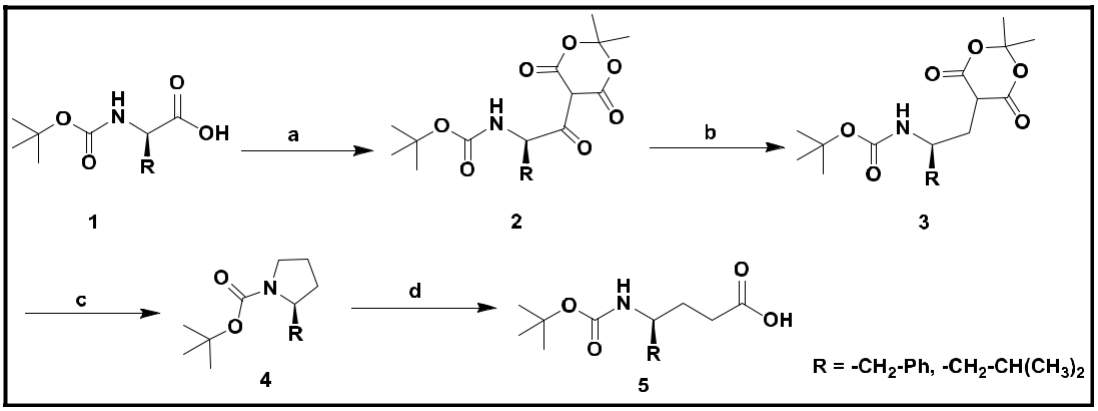

Reagents and condtions: a) Dry DCM, Meldrum's acid, DMAP, EDC 0°C to rt, 8 h; b) Dry DCM, CH_3COOH, $NaBH_4$, 0°C to rt, 1 h; c) Toluene, reflux, 1 h; (d) MeOH, 2N-NaOH, 1 h, rt.

Synthesis of hybrid peptides P1-P8:

Synthesis of LA-Lys (Cbz)-PEA, **P1:**

Boc-Lys (Cbz)-OH (1.14g, 3.0mmol) was dissolved in 5.0ml of DCM was added NMM (0.5ml, 5 mmol) followed by the addition of EDC (0.573g, 3.0mmol) and phenethyl-amine (PEA) (0.6ml, 5.0mmol) at 0^{o}C and stirred the reaction mixture for 12h. The progress of the reaction was monitored using TLC at regular intervals. The solvent was evaporated and the residue was extracted with ethyl acetate and was washed successively with 2N-HCl (3×10ml), 2M-Na_2CO_3 (3×10ml) and brine solution. The combined organic layer was dried over anhydrous sodium sulphate and evaporated under vacuum to yield Boc-Lys (Cbz)-PEA

(**1**), which was deprotected using 30% TFA in DCM to yield the peptide free base H_2N-Lys (Cbz)-PEA [29].

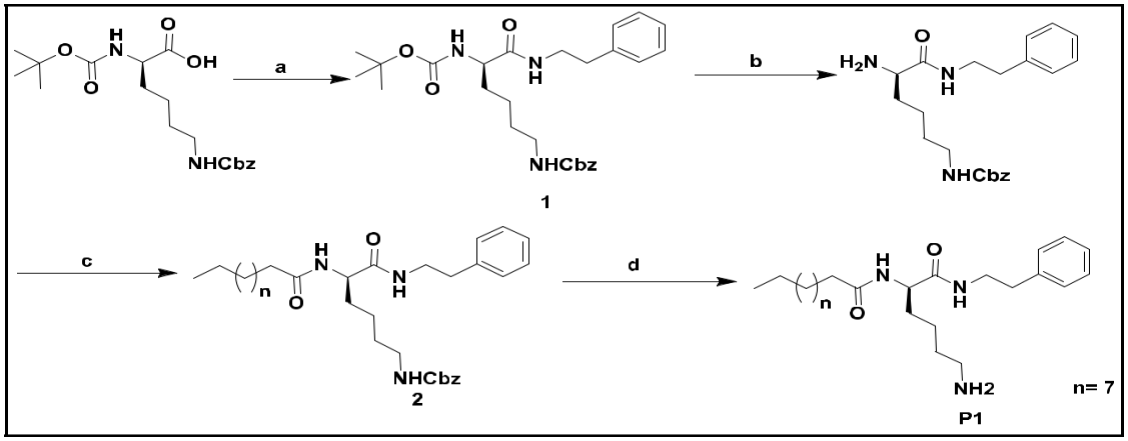

Reagents and conditions: a) Dry DCM, NMM, EDC, PEA, 0^{o}C to rt, 12 h; b) TFA in DCM, 2 h; c) Dry DMF, NMM, EDC, HOBt, Lauric acid, 0^{o}C to rt, 24 h; d) 10% Pd/C in dry MeOH, 12h.

Synthesis of hybrid peptides P2-P6:

Scheme.3

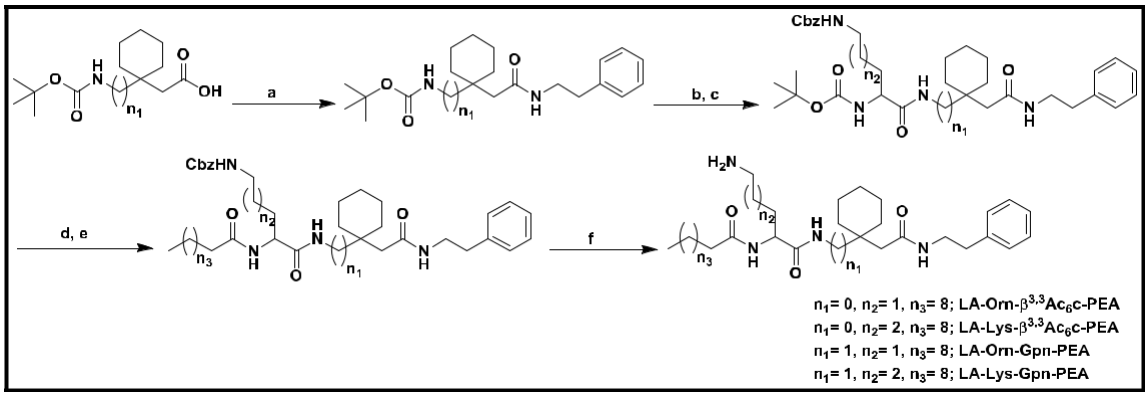

N-(6-amino-1-oxo-1-((1-(2-oxo-2-(phenethylamino) ethyl cyclohexyl amino) hexan-2-yl) dodec anamid, P2:

^{1}H NMR (400 MHz, DMSO): δ 7.95 (d, J = 6.0 Hz, 1H), 7.68 (s, 1H), 7.28 (m, 3H), 7.20 (m, 3H), 4.17 (m,1H), 3.27 (m, 2H), 2.72 (dd, J = 14.0, 6.8 Hz, 3H), 2.35 (d, J = 13.1 Hz, 1H), 2.17–2.10 (m, 3H), 2.02 (d, J = 11.5 Hz, 6H), 1.71–1.09 (m, 34H), 0.85 (d, J = 6.1 Hz, 3H).^{13}C NMR (126 MHz, $CDCl_3$): δ 174.22, 172.29, 172.25, 170.80, 139.08, 128.83, 128.80, 128.58, 128.55, 126.45, 55.31, 53.72, 40.63, 39.20, 36.39, 36.32, 35.41, 35.05, 34.67, 31.94, 31.52, 29.71, 29.67, 29.61, 29.51, 29.41, 29.39, 26.56, 25.80, 25.31, 22.70, 22.30, 21.68, 14.17, 14.13. HRMS-ESI: M_{Cal}= 570.44; M_{Obs}=571.45$[M+H]^+$.

N-(5-amino-1-oxo-1-((1-(2-oxo-2-(phenethylamino) ethyl) cyclohexyl) amino) pentan-2-yl) dodecanamide, P3:

^{1}H NMR (400 MHz, $CDCl_3$): δ 7.26 (m,5H), 7.00 (d, J = 5.9 Hz, 1H), 6.35 (s, 1H), 6.23 (s, 1H), 4.16 – 4.08 (m, 1H), 3.58 (m, 2H), 3.41 (m, 1H), 2.81 (dd, J = 15.2, 7.8 Hz, 4H), 2.70 (d, J = 13.4 Hz, 2H), 2.19 (m, 3H), 1.33 (m, 30H), 0.88 (t, J = 6.3 Hz, 3H).^{13}C NMR (126 MHz, $CDCl_3$): δ 173.67, 171.74, 170.51, 139.23, 128.88, 128.52, 126.41, 55.07, 53.54, 53.48, 45.03, 41.20, 40.40, 36.59, 36.53, 35.45, 35.02, 34.82, 31.88, 30.10, 29.65, 29.64, 29.54,

29.40, 29.37, 29.35, 28.13, 25.79, 25.74, 25.35, 22.71, 21.71, 21.64, 14.30. HRMS-ESI: M_{Cal}=5576.43; M_{Obs}=557.44$[M+H]^+$.

N-(6-amino-1-oxo-1-(1-(2-oxo-2-(phenethyl amino) ethyl) cyclohexyl) methyl) amino) hex an-2-yl) dodecanamide, P4:
^{1}H NMR (400 MHz, $CDCl_3$): δ 7.96 (s, 1H), 7.24 (m, 5H), 7.03 (d, *J* = 6.9 Hz, 1H), 4.54 (s, 1H), 3.50 (t, *J* = 9.6 Hz, 2H), 3.21 (dd, *J* = 13.5, 6.2 Hz, 1H), 3.09 (dd, *J* = 13.6, 5.7 Hz, 1H), 3.01 (s, 1H), 2.85 (t, *J* = 6.9 Hz, 2H), 2.25 (t, *J* = 7.4 Hz, 2H), 2.10 (s, 2H), 1.60 (s, 3H), 1.54 – 1.16 (m, 30H), 0.87 (t, *J* = 6.3 Hz, 3H).^{13}C NMR (101 MHz, $CDCl_3$): δ 174.40, 172.18, 171.41, 139.09, 128.80, 128.45, 126.32, 52.59, 45.73, 43.01, 40.58, 40.35, 37.23, 36.59, 35.61, 34.27, 34.15, 31.90, 31.35, 29.64, 29.62, 29.53, 29.38, 29.34,25.92, 25.74, 24.85, 22.81, 22.60, 21.53, 14.11. HRMS-ESI: M_{cal}= 584.4649, M_{obs}=585.4722$[M+H]^+$.

N-(5-amino-1-oxo-1-(1-(2-oxo-2 (phenethyl amino) ethyl) cyclohexyl) methyl) amino) pent an-2-yl) dodecan amide, P5:
^{1}H NMR (400 MHz, $CDCl_3$): δ 7.71 (s, 1H), 7.25 (m, 5H), 6.50 (d, *J* = 7.7 Hz, 1H), 4.50(m, 1H), 3.59 – 3.49 (m, 3H), 3.22 (dd, *J* = 13.6, 6.5 Hz, 2H), 3.07 (dd, *J* = 13.6, 6.0 Hz, 2H), 2.85 (t, *J* = 6.9 Hz, 3H), 2.38 (d, *J* = 6.2 Hz, 2H), 2.20(m, 3H), 2.05 (m,3H), 1.25 (s, 31H), 0.87 (t, *J* = 6.5 Hz, 3H).^{13}C NMR (126 MHz, $CDCl_3$): δ 174.78, 174.28, 172.74, 140.48, 130.24, 129.90, 127.78, 54.87, 54.60, 53.43, 42.03, 38.64, 38.18, 37.11, 35.93, 35.61, 34.34, 33.34, 31.09, 31.07, 31.00, 30.92, 30.86, 30.83, 30.79, 28.45, 27.37, 27.31, 24.78, 24.12, 22.95, 15.57. HRMS-ESI: M_{Cal}=570.44; M_{Obs}=571.45$[M+H]^+$.

N-(6-amino-1-oxo-1-((5-oxo-5-(phenethylamino)-1-phenylpentan-2-yl) amino) hexan-2-yl) dodecanamide, P6:
^{1}H NMR (400 MHz, $CDCl_3$): δ 7.33–7.07 (m, 10H), 6.61 (s, 1H), 6.54 (d, *J* = 8.1 Hz, 1H), 6.24 (d, *J* = 7.0 Hz, 1H), 4.24 (q, *J* = 6.7 Hz, 6.7 Hz, 1H), 4.01 (s, 18H), 3.55 (m, 2H), 3.42 (m, 2H), 2.82(t, *J* = 6.5 Hz, 3H), 2.69 (dd, *J* = 13.7, 7.1 Hz, 2H), 1.83 – 1.63 (m, 3H), 1.54 (d, *J* = 28.3 Hz, 4H), 1.35 – 1.15 (m, 21H), 0.87 (d, *J* = 6.7 Hz, 3H).^{13}C NMR (126 MHz, $CDCl_3$): δ 173.80, 171.77, 156.30, 138.68, 136.33, 128.73, 128.59, 128.53, 128.11, 128.05, 126.53, 66.54, 52.78, 40.67, 40.41, 36.40, 35.48, 31.92, 29.65, 29.63, 29.55, 29.49, 29.39, 29.36, 29.32, 25.66, 22.70, 22.37, 14.15. HRMS-ESI: M_{cal}= 606.44; M_{Obs}=607.45$[M+H]^+$.

Synthesis of peptides P7 and P8:
Boc-Lys (Cbz)-OH (3.0mmol) was dissolved in 5.0 ml of DCM was added NMM followed by the addition of EDC (3.0mmol) and PEA (5.0mmol) at 0^{o}C and stirred the reaction mixture for 12 h. The progress of the reaction was monitored using TLC at regular intervals. The solvent was evaporated and the residue was extracted with ethyl acetate and was washed successively with 2N-HCl (3×10ml), 2M-Na_2CO_3 (3×10ml) and brine solution. The combined organic layer was dried over anhydrous sodium sulphate [30].

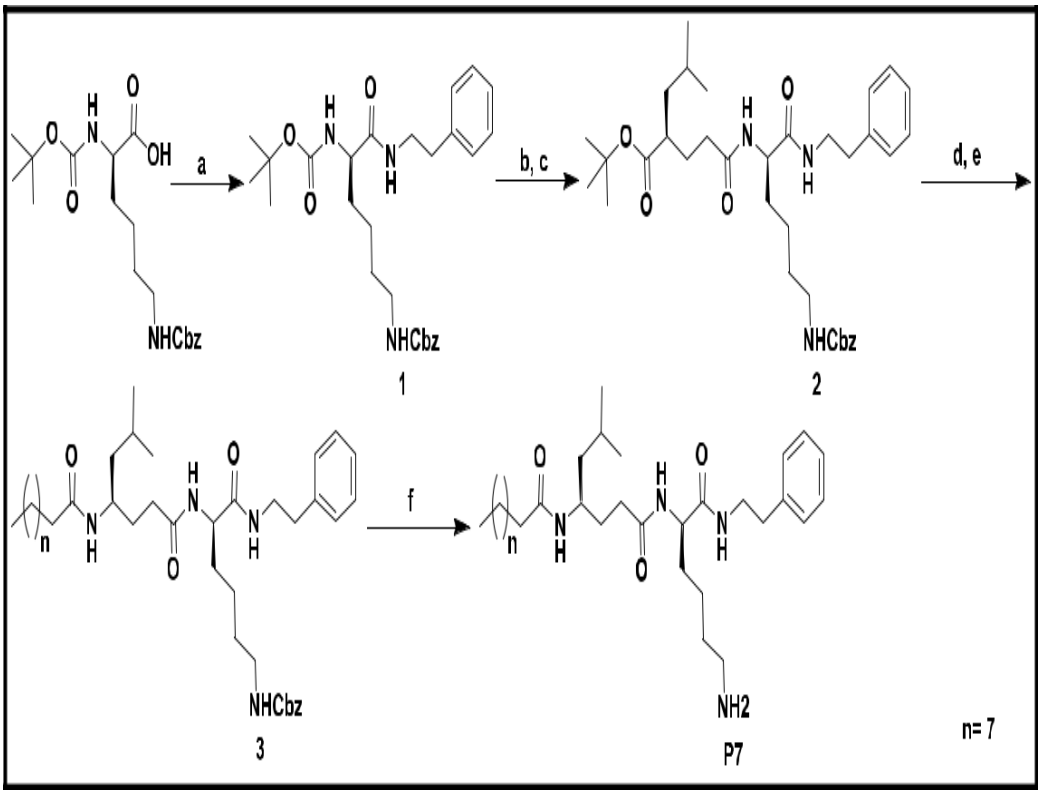

N-(1-(6-amino-1-oxo-1-(phenethylamino) hexan-2-yl) amino)-6-methyl-1-oxoheptan-4-yl) dodecanamide, P7:

^{1}H NMR (400 MHz, $CDCl_3$): δ 7.26-7.18 (m, 5H), 6.92 (s, 1H), 5.96 (d, *J* = 8.0Hz, 1H), 5.72 (s, *J* = 8Hz, 1H), 4.39 (s, 1H), 3.93 (s, 1H), 3.45 (s, 3H), 2.80 (s, 3H), 2.54 (s, 3H), 2.18 (s, 3H), 1.61 (s, 8H), 1.25 (s, 21H), 0.88 (s, 9H).^{13}C NMR (101 MHz, $CDCl_3$): δ 202.45, 196.30, 172.96, 128.78, 128.74, 128.42, 126.29, 126.26, 69.02, 66.84, 63.82, 53.38, 47.05, 46.87, 46.75, 40.83, 40.52, 40.30, 40.10, 40.09, 39.88, 36.91, 35.66, 35.61, 33.05, 33.01, 32.94, 32.88, 31.88. HRMS-ESI: M_{Cal}=572.46; M_{Obs}=573.47$[M+H]^+$.

N-(1-acetyl-4-(2-(6-amino-1-oxo-1-(phenethylamino) hexan-2-yl) amino)-2-oxoethyl) piperi din-4-yl) dodecanamide, P8:

^{1}H NMR (400 MHz, $CDCl_3$): *δ* 7.33–7.13 (m, 6H), 6.81 (s, 1H), 6.26 (s, 1H), 4.29 (s, 1H), 4.14 (s, 1H), 3.6–3.29 (m, 5H), 3.27 (d, *J* = 6.5 Hz, 1H), 2.97 (dd, *J* = 30.4, 13.6 Hz, 1H), 2.76 (m, 2H), 2.74–2.64 (m, 1H), 2.63-2.48 (m, 1H), 2.38 (s, 1H), 2.14 (m, 3H), 2.08 (d, *J* = 2.7 Hz, 1H), 2.06 (s, 3H), 1.58 (m, 9H), 1.24 (s, 19H), 0.88 (s, 3H).^{13}C NMR (126 MHz, $CDCl_3$): δ 174.28, 171.70, 169.12, 138.95, 128.79, 128.77, 128.73, 128.68, 128.59, 128.55, 128.51, 128.20, 126.36, 53.47, 53.45, 53.38, 53.34, 53.33, 53.29, 40.80, 37.41, 35.63, 31.93, 29.70, 29.65, 29.60, 29.49, 29.38, 25.83, 22.69, 21.41, 14.17. HRMS-ESI: M_{Cal}= 613.45; M_{Obs}=614.46$[M+H]^+$.

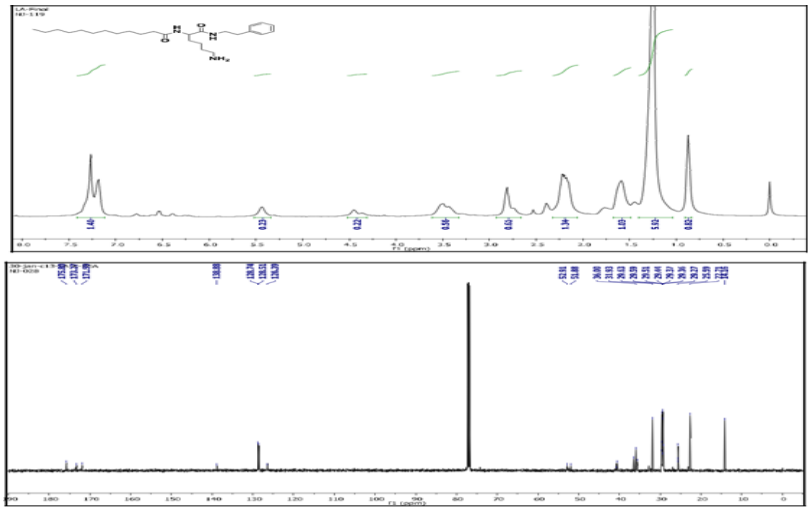

Fig.24: 1H and 13C NMR of LA-Lys-PEA, P1

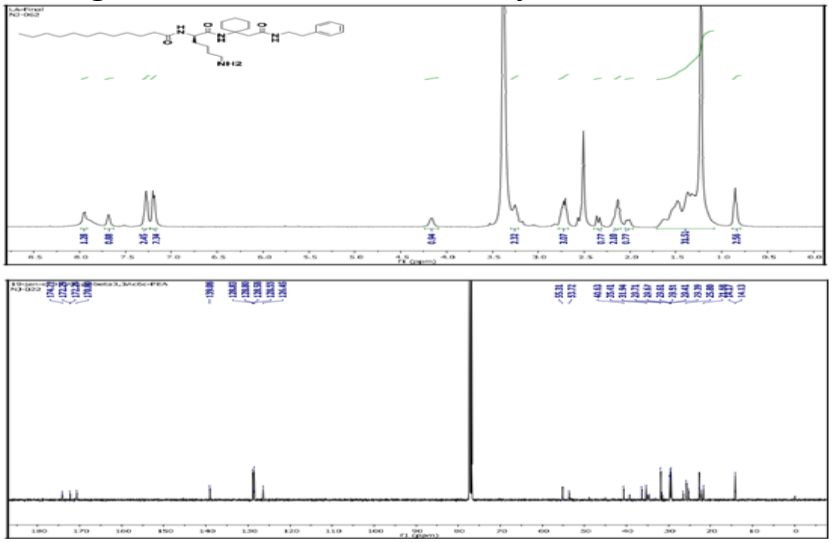

Fig.25: 1H and 13C NMR of LA-Lys-3,3Ac6c-PEA, P2 in DMSO-d6

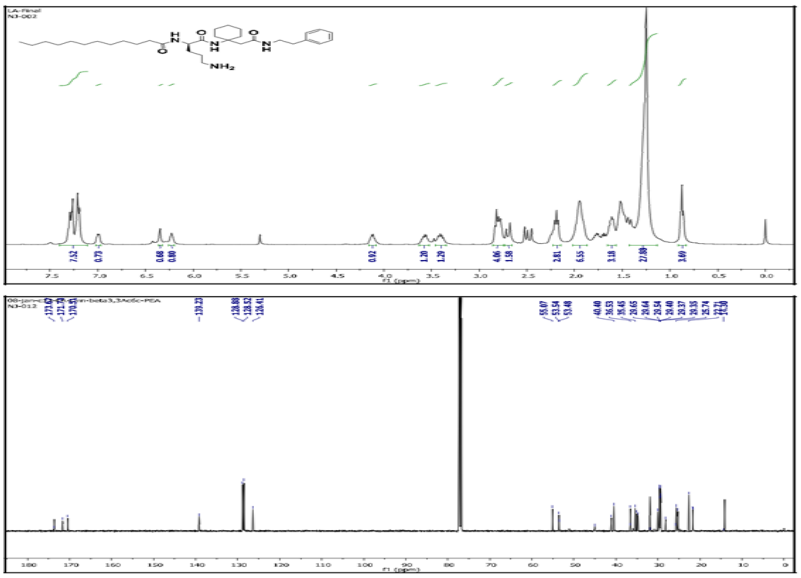

Fig.26: 1H and 13C NMR of LA-Orn-□3,3Ac6c-PEA, P3 in DMSO-d6

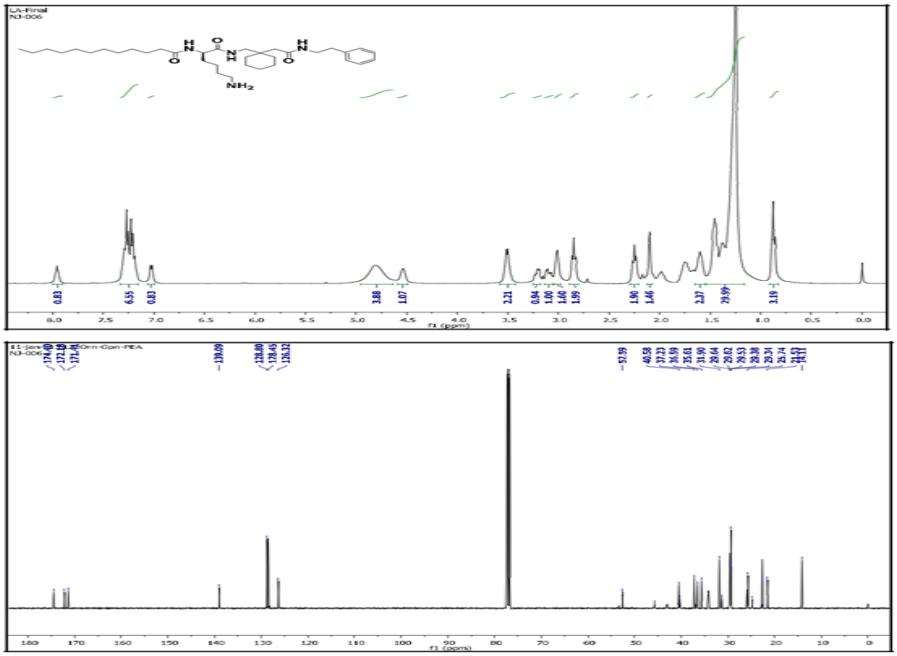

Fig.27: 1H and 13C NMR of LA-Lys-Gpn-PEA, P4 in DMSO-6

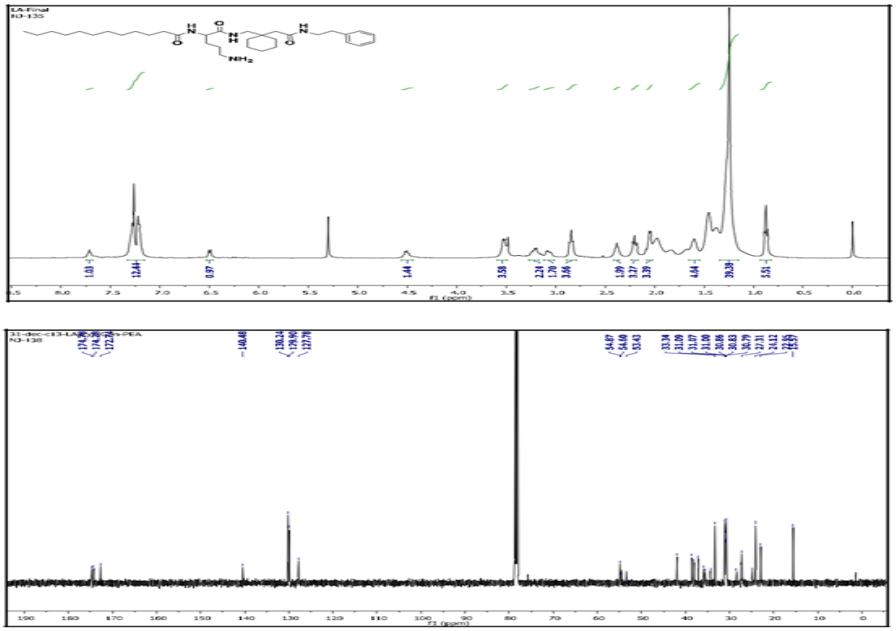

Fig.28: 1H and 13C NMR of LA-Orn-Gpn-PEA, P5

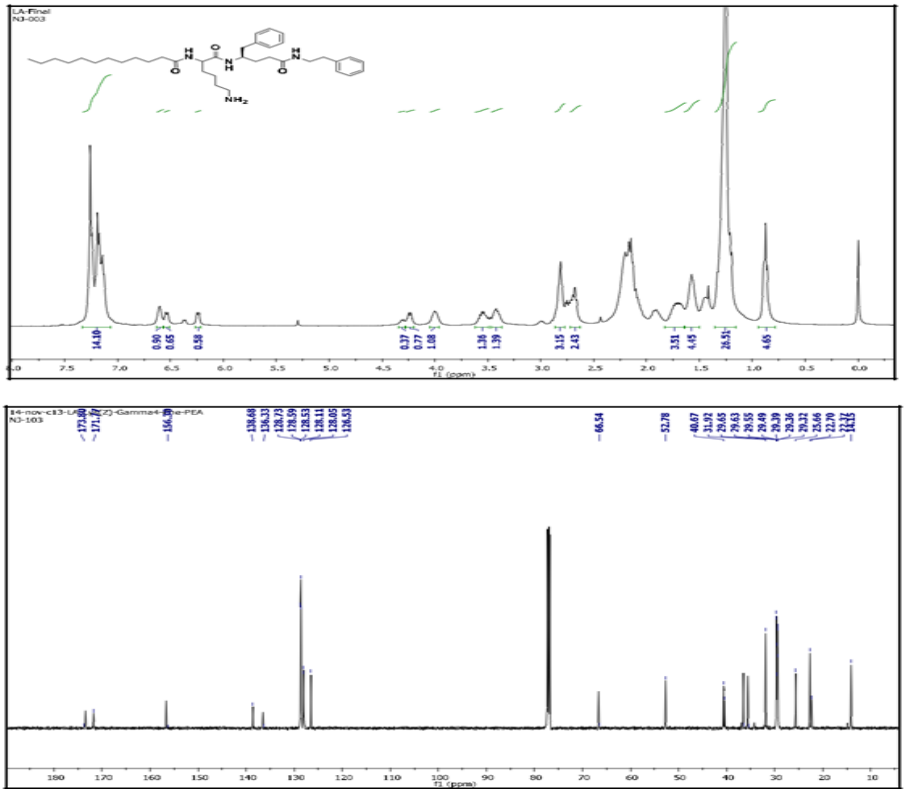

Fig.29: 1H and 13C NMR of LA-Lys-C4 -L-Phe-PEA, P6

Antimicrobial activity of hybrid peptides:

To determine the antimicrobial activity of the peptides, MIC and MBC values were evaluated by broth microdilution against *Bacillus subtilis* (MTCC 121*), Pseudomonas aeruginosa* (MTCC 424), *Salmonella typhimurium* (MTCC 98), *Escherichia coli* (MTCC118), *Klebsiella pneumonia* (MTCC 109), *Staphylococcus aureus* (MTCC 737) by method described by Clinical Laboratory and Standards Institute (CLSI) with slight modification (Steinberg *et al* 1997). Briefly, the bacterial colonies were grown in Mueller-Hinton broth medium to mid logarithmic phase then bacteria were adjusted to a 0.5 McFarland turbidity standard with OD at 600nm to 0.321 which corresponds to 1.5 $x10^8$ CFU/mL followed by serial dilutions to give 4 $x10^4$ CFU/mL. The 50µL aliquots of these bacteria were added to 96 well flat bottom microtiter plates containing 150µL of peptides at different concentration (50µM, 25µM, 12.5µM, 6.25µM, 3.12µM, 1.56µM and 0.78µM) and mixture were incubated at 37ºC for 12-16 h. Appropriate positive (Streptomycin) and blank controls (virgin media) were used. For determining MIC and MBC, the 50µL of sample was taken from well having non-visible growth was spread on MH agar plates and incubated overnight at 37°C. The lowest concentration at which there was no visible growth was considered as minimum inhibitory concentration (MIC). For determining MBC, the 50µL of sample was taken from well having non-visible growth was spread on MH agar plates and incubated overnight at 37°C. The lowest concentration at which 99.9% of the pathogen was killed was considered as the minimum bactericidal concentration (MBC).

Time kill kinetics assay:

P. aeruginosa and *S. aureus* were grown to mid logarithmic phase and then diluted to 10^4 CFU/ml suspensions. The diluted bacterial suspension was incubated with different concentration of peptides **P2**, **P3**, **P4**, **P5** and **P6** for 10, 30, 60 and 120 min respectively. After the incubation, the mixture was diluted to 10^2 times and spread on MH agar plates. After incubation at 37 ºC for 24 h, the number of colonies was counted (Choi *et al* 2009).

Fluorescence microscopy:

The effect of peptides (**P2**, **P3**, **P4** and **P5**) on bacterial membrane integrity of *P. aeruginosa* and *S. aureus* was assessed by fluorescence microscopy using 4′,6-diamidino-2-phenylindole dihydrochloride (DAPI) and propidium iodide (PI). PI can only pass through damaged membrane and therefore stain only dead cells whereas DAPI is able to dye all bacteria cells regardless of their viabilities. The bacterial cultures were grown to mid logarithmic phase and incubated with peptide **P3** and **P5** with 8 μM concentrations at 37°C for 2 h. The cells were collected by centrifugation at 5000 g for 15 min, washed with PBS then incubated with PI (5 μg/mL) for 15 min at 0°C in dark. Unbound PI was removed by washing the cells with PBS. Then cells were incubated with DAPI (10 μg/mL) for 15 min at 0°C in dark. The cultures without peptide treatment were designated as controls. The stained bacteria were observed under an inverted microscope equipped with digital camera (Olympus Imaging Corp., Center Valley, PA, USA) (Li *et al* 2013).

Hemolytic assay:

The hemolytic activity means amount of hemoglobin released by the lysis of human erythrocytes (Conlon *et al* 2003). The human red blood cells (RBC) were freshly collected and washed with sterile phosphate buffered saline (PBS) and centrifuged at 1000 g for 10 min at 4ºC until the upper solution became clear. RBCs were diluted to 5% suspension and mixed with peptides at different concentrations (500 to 7.81 μM) in a 96 well plate. PBS and 0.1% Triton X-100 were used as negative and positive controls, respectively. The mixture was incubated at 37ºC for 1 h and centrifuged at 2000 rpm for 20 min. The supernatant was transferred to a 96 well plate and absorbance was measured at 360 nm on Microplate Spectrophotometer (Thermo Scientific Multiskan GO Microplate Spectrophotometer). The percentage of hemolysis was calculated using the following formula: 100% hemolysis = 100 ($Abs_{peptide}$-Abs_{PBS}) / ($Abs_{triton\ X}$-Abs_{PBS})

All the peptides **P1-P8** were evaluated for the antimicrobial activity against Gram-positive *Staphylococcus aureus* (MTCC 737), *Bacillus subtilis* (MTCC 121), *Salmonella typhimurium* (MTCC 98) and Gram-negative *Klebsiella pneumonia* (MTCC 109), *Pseudomonas aeruginosa* (MTCC 424) and *Escherichia coli* (MTCC 118) bacterialstrains. The *in vitro* antimicrobial activities of all the peptides are listed in Table 3.1. Among all, peptides **P2**, **P3**, **P4** and **P5** exhibited potent antimicrobial activities against Gram-negative bacteria, *P. aeroginosa* (MIC: 6.25 μM). In addition, peptides **P2, P3** and **P5** showed the antimicrobial activities against Gram-positive bacteria, *S. aureus* (MIC: 6.25 μM). To understand the efficacy of peptides, time kill assay was used to investigate the ability of peptides **P2**, **P3, P4, P5** and **P6** to kill both *S. aureus* (MTCC 737) and *P.aeruginosa.* Time kill assay was used to investigate the ability of hybrid peptides **P2**, **P3, P4** and **P5** to kill both Gram-positive *S. aureus* (MTCC 737) & Gram-negative *P.aeruginosa* (MTCC 424) bacteria. These peptides were tested at concentration equal to 0.5xMIC, MIC and 2xMIC. After two hours of treatment, the cell viability was determined by:

Table.5: Antimicrobial activity of hybrid peptides (**P1-P8**). Microorganisms used were *Staphylococcus aureus* MTCC 737; *Bacillus subtilis* MTCC 121; *Salmonella typhimurium* MTCC 98; *Klebsiella pneumonia* MTCC 109; *Pseudomonas aeruginosa* MTCC 424; *Escherichia coli* MTCC 118; Streptomycin (µg/mL) and blank (virgin media) were used as positive and negative control

Pathogen	**Staphylococcus aureus**	**Bacillus subtilis**	**Salmonella typhimurium**	**Klebsiella pneumonia**	**Pseudomonas aeruginosa**	**Escherichia coli**
Compound	MICa	MBCb	MIC	MBC	MIC	MBC
P1	>50	-	25	50	-	50
P2	6.25	12.5	-	12.5	-	12.5
P3	6.25	12.5	-	25	-	12.5
P4	25	50	12.5	-	12.5	-
P5	6.25	-	12.5	-	12.5	25
P6	12.5	25	-	25	12.5	-
P7	25	50	50	-	50	-
P8	50	-	-	>50	>50	-
Streptomycin	-	0.623	-	0.623	-	0.623

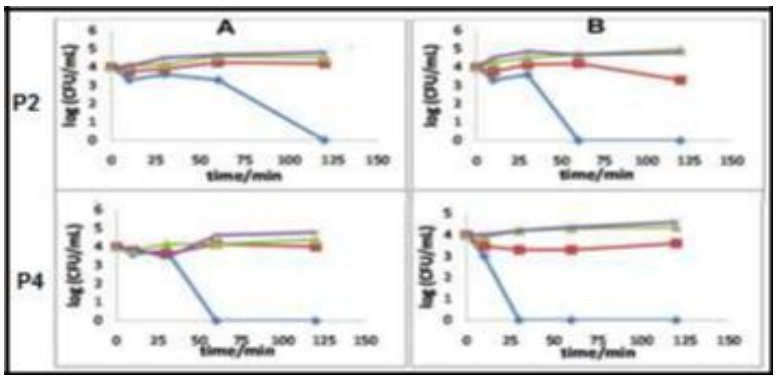

Fig.30: Time-kill curves of peptides **P2** and **P4** for A) *P. aeruginosa* B) *S. aureus*. The killing activity of peptides against these strains was monitored for the first 2 h. The peptide concentration used in the experiment were untreated control (purple), 0.5 MIC (green), MIC (red) and 2x MIC (blue).

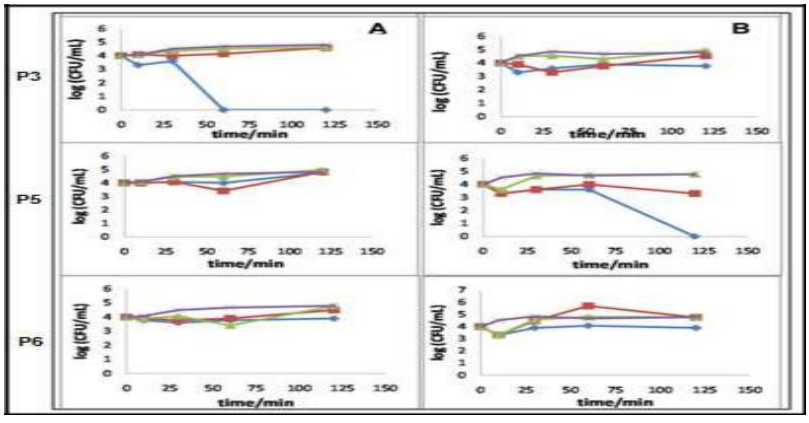

Fig.31: Time-kill curves of **P3**, **P5** and **P6** for A) *P. aeruginosa* B) *S. aureus* respectively. The killing activity of peptides against these strains was monitored for the first 2 h. The peptide concentration used in the experiment were untreated control (purple), 0.5 MIC (green), MIC (red), and 2x MIC (blue).

Fig.30 and 31 show the fluorescence micrograph of *P. aeruginosa* and *S. aureus* after treatment for 2 h. As shown in Figure.10 the treatment of bacteria with peptides **P2** and **P4** resulted in visibility of red-fluorescent bacteria under the PI channel,suggesting the membranes of both *P. aeruginosa* and *S. aureus* were damaged. In addition, the treatment with **P3** and **P5** led to significant aggregation of *S. aureus* is believed to arise from dissipation of membrane potential due to membrane disruption as shown (Wu *et al* 2012, Padhee *et al* 2014).

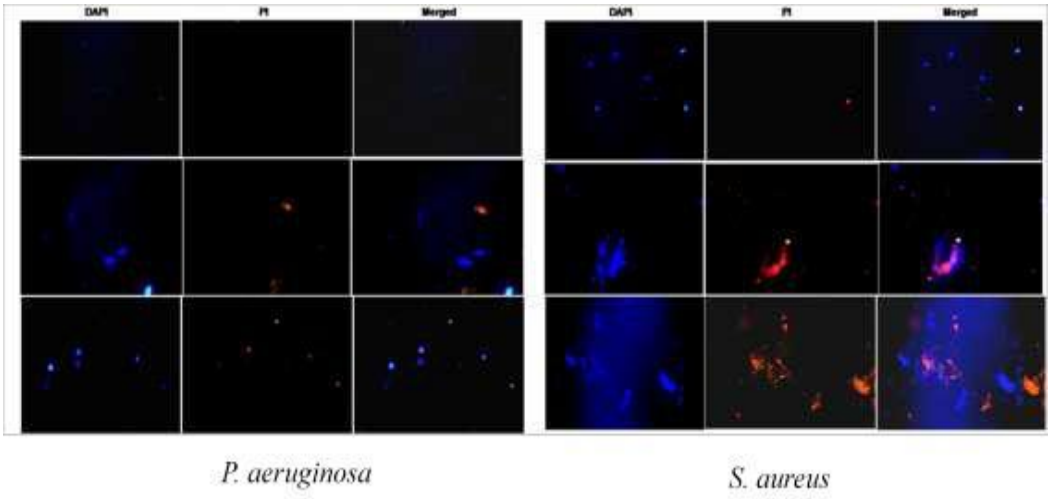

Fig.32: Fluorescence micrographs of *P. aeruginosa.* 1st row: untreated control; 2nd row: treated with 8µM of **P2** for 2 h; 3rd row: treated with 8µM of **P4** for 2 h. & *S. aureus.* 1st row: untreated control; 2nd row: treated with 8 µM of **P2** for 2 h; 3rd row: treated with 30 µM of **P4** for 2 h.

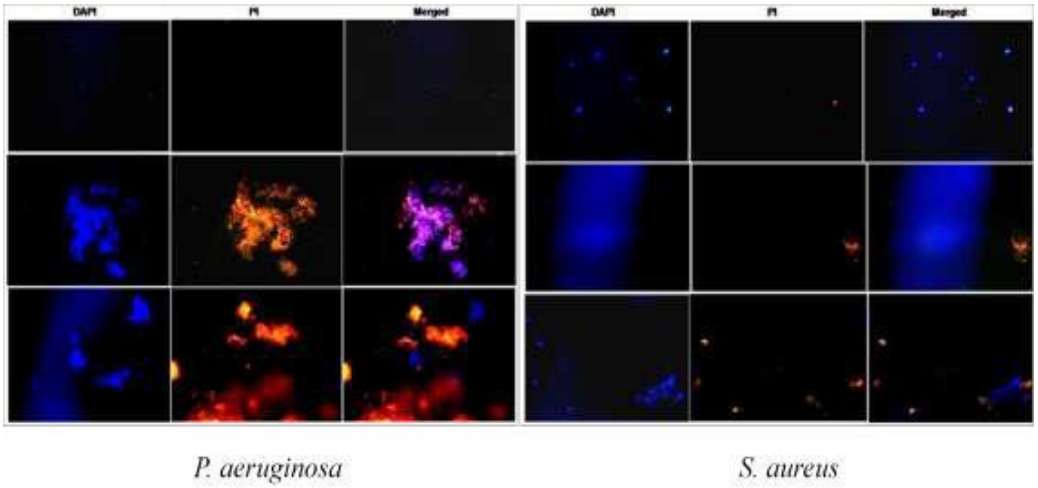

Fig.33: Fluorescence micrographs of *P. aeruginosa* Row 1) untreated control 2) treated with 8 µM of **P3** 3) treated with 4µM of **P5** and *S. aureus* Row 1) untreated control 2) treated with 8 µM of **P3** 3) treated with 8µM of **P5**.

Further, all the peptides were checked for their haemolytic properties at different concentration. The haemolytic activities, i.e. the concentration needed to induce 50% (HC_{50}) and 10% (HC_{10}) haemoglobin release of all the peptides are summarized in Table.6. Among all the active peptides, peptide **P4** exhibited lowest haemolytic activity at HC_{50} and $HC_{10.}$

Table.6: Hemolytic activity (μM) of hybrid peptides **P1-P8**

Compound	HC_{50}	HC_{10}
P1	253.42	77.98
P2	29.57	<7.812
P3	81.07	<7.812
P4	**>500**	**175.06**
P5	78.05	<7.812
P6	203.62	<7.812
P7	>500	308.64
P8	>500	313.45

Conclusion

This study focused on the synthesis and conformational analysis of α, β hybrid peptides containing a conformationally constrained β, β-Disubstituted-β-amino acid, β3, 3-Ac6c, both in solution and in crystal form. NMR studies confirmed the folded structures of peptides P2-P4 in solution. The crystal structures of peptides P2 and P3 revealed the presence of C11/C9 intermolecular hydrogen bonds with opposite directionality. These findings demonstrate that the cyclohexyl constraint at the Cβ position of β-amino acids allows for the formation of helical structures, with the cyclohexane ring adopting a chair conformation in all the peptides. Furthermore, the antimicrobial properties of short hybrid peptides containing β- and γ-amino acids were investigated. The peptides incorporating β, β-Disubstituted-β-amino acid (β3,3-Ac6c) and β, β-disubstituted-γ-amino acid (Gpn) along with lysine (Lys) displayed rapid antimicrobial activity and membrane disruption against both Gram-positive (S. aureus) and Gram-negative (P. aeruginosa) pathogens. Notably, peptide P4 exhibited the lowest hemolytic activity among all the active peptides tested. These findings suggest that the introduction of β, β-disubstituted-β-amino acid and β, β-disubstituted-γ-amino acids into shorter peptide sequences holds promise for the development of potent antimicrobial agents. Overall, this study highlights the potential of incorporating conformationally constrained amino acids in hybrid peptides to enhance their antimicrobial properties, paving the way for further research and the development of novel antimicrobial agents.

References:

1. Smith, J. K., & Johnson, A. B. "Peptide isosteres: Tools for drug discovery." Expert Opinion on Drug Discovery, vol. 10, no. 7, pp. 713-726, 2015.
2. Bowers, A. A., & Klevit, R. E. "Backbone mimicry in protein-protein interactions." Trends in Biochemical Sciences, vol. 40, no. 7, pp. 347-354, 2015.
3. Ghadiri, M. R., & Fernández-López, S. "Mimicking the dynamic nature of proteins: Peptide-based synthetic receptors and catalysts." Current Opinion in Chemical Biology, vol. 3, no. 6, pp. 672-677, 1999.
4. White, C. J., et al. "Peptide-based therapeutic approaches for modulating protein-protein interactions." Medicinal Chemistry Communications, vol. 6, no. 1, pp. 50-61, 2015.

5. Lu, Y., & Chen, S. C. "Revisiting an old peptide bond surrogate: Amide esters." Chemical Society Reviews, vol. 42, no. 11, pp. 4562-4573, 2013.
6. Kent, S. B. "Chemical synthesis of peptides and proteins." Annual Review of Biochemistry, vol. 57, pp. 957-989, 1988.
7. P. Bhatt et al., "Functional and Tableting Properties of Alkali-Isolated and Phosphorylated Barnyard Millet (Echinochloa esculenta) Starch," ACS omega, Aug. 2023, doi: https://doi.org/10.1021/acsomega.3c03158.
8. Bracken, C., et al. "Amide bond isosteres: Replacement of a peptide bond by a urea or thiourea bond." Journal of Medicinal Chemistry, vol. 41, no. 18, pp. 3427-3436, 1998.
9. Rollin, P., et al. "Structural features of peptide isosteres: Guidelines for design and synthesis." Chemical Society Reviews, vol. 44, no. 14, pp. 4368-4403, 2015.
10. S. Singh, P. Bhatt, S. K. Sharma, and S. Rabiu, "Digital Transformation in Healthcare: Innovation and Technologies," in Blockchain for Healthcare Systems, Boca Raton: CRC Press, 2021, pp. 61–79.
11. P. Bhatt et al., "Plasma modification techniques for natural polymer-based drug delivery systems," Pharmaceutics, vol. 15, no. 8, 2023.
12. Rana, T. M. "Modification of peptides and proteins by amide bond mimics." Current Opinion in Chemical Biology, vol. 4, no. 5, pp. 592-596, 2000.
13. Minko, T., et al. "Peptide-based multifunctional nanomaterials." Scientific Reports, vol. 8, no. 1, Article number: 3359, 2018.
14. P. Bhatt, A. Kumar, and R. Shukla, "Nanorobots Recent and Future Advances in Cancer or Dentistry Therapy- A Review," American Journal of PharmTech Research, vol. 9, no. 3, pp. 321–331, Jun. 2019, doi: https://doi.org/10.46624/ajptr.2019.v9.i3.027.
15. Blondelle, S. E., & Houghten, R. A. "Design of model peptides: Applications to antimicrobial peptides and vaccine development." Journal of Peptide Science, vol. 3, no. 5, pp. 275-282, 1997.
16. Goodman, M., & Raghu-Varma, P. "Strategies for the design of nonpeptidic peptide mimetics." Accounts of Chemical Research, vol. 25, no. 11, pp. 341-349, 1992.
17. Gellman, S. H. "Foldamers: A manifesto." Accounts of Chemical Research, vol. 31, no. 3, pp. 173-180, 1998.
18. S. K. Sharma and P. Bhatt, "Controlled release of bi-layered EGCG tablets using 3D printing techniques," J. Pharm. Res. Int., pp. 5–13, 2021.
19. Patch, J. A., & Barron, A. E. "Helical peptoid mimics of magainin-2 amide." Journal of the American Chemical Society, vol. 124, no. 48, pp. 14122-14123, 2002.
20. Jung, D., et al. "Peptidomimetic therapeutics: Scientific approaches and opportunities." Drug Discovery Today, vol. 16, no. 11-12, pp. 506-516, 2011.
21. P. Bhatt, S. Singh, S. K. Sharma, and V. Kumar, "Blockchain technology applications for improving quality of electronic healthcare system," in Blockchain for Healthcare Systems, Boca Raton: CRC Press, 2021, pp. 97–113.
22. Bock, J. E., & Gough, G. R. "Chemical peptide synthesis: Strategies and tools for the new millennium." Biopolymers, vol. 55, no. 3, pp. 229-259, 2000.
23. Wilson, D. S., & Keefe, A. D. "Random peptide libraries: A source of specific protein binding molecules." Current Opinion in Chemical Biology, vol. 2, no. 6, pp. 668-674, 1998.
24. C. Goyal, P. Bhatt, S. Rawat, V. Sharma, and Meena Rani Ahuja, "Estimation of shelf-life of Balachaturbhadrika syrup containing different sweetening agents," Research journal of pharmacy and technology, pp. 5078–5083, Nov. 2022, doi: https://doi.org/10.52711/0974-360x.2022.00853.

25. M. K. Malik, P. Bhatt, J. Singh, R. D. Kaushik, G. Sharma, and V. Kumar, "Preclinical safety assessment of chemically cross-linked modified mandua starch: Acute and sub-acute oral toxicity studies in Swiss albino mice," ACS Omega, vol. 7, no. 40, pp. 35506–35514, 2022.
26. M. K. Malik, V. Kumar, J. Singh, P. Bhatt, R. Dixit, and S. Kumar, "Phosphorylation of alkali extracted mandua starch by STPP/STMP for improving digestion resistibility," ACS Omega, vol. 8, no. 13, pp. 11750–11767, 2023.
27. Hruby, V. J., et al. "Peptide conformation in drug design and discovery." Chemical Reviews, vol. 101, no. 12, pp. 3273-3508, 2001.
28. Brunsveld, L., et al. "Supramolecular polymers." Chemical Reviews, vol. 101, no. 12, pp. 4071-4097, 2001.
29. Heinis, C. "Rationally designed peptide macrocycles." Current Opinion in Chemical Biology, vol. 38, pp. 45-51, 2017.